University of Nevada, Reno

Development of an Aerosol Testing Chamber for Mining Environments and Evaluation of New Silica Dust Mass Concentration Methods Using the NIOSH FTIR Standard Technique

A thesis submitted in partial fulfillment of the

requirements for the degree of Master of Science in

Mining Engineering

By

Pedro Nascimento

Drs. Charles Kocsis/Thesis Advisor

W. Patrick Arnott/Thesis Co-advisor

August, 2021

THE GRADUATE SCHOOL

We recommend that the thesis
prepared under our supervision by

PEDRO NASCIMENTO

Entitled

Development of an Aerosol Testing Chamber for Mining Environments and Evaluation of New Silica Dust Mass Concentration Methods Using the NIOSH FTIR Standard Technique

be accepted in partial fulfillment of the
requirements for the degree of

MASTER OF SCIENCE IN MINING ENGINEERING

Charles Kocsis, Ph.D.
Advisor

Raj R. Kallu, Ph.D.
Committee Member

W. Patrick Arnott, Ph.D.
Graduate School Rep.

David W. Zeh, Ph.D., Dean
Graduate School

August 2021

Abstract

Respirable crystalline silica (RCS) and respirable coal dust are a health hazard for industrial workers, mainly in the mining industry, which has to be monitored and have their concentration controlled under permissible limits. Innumerous techniques for silica and coal monitoring have been applied in mining environments, but most of them with the shortcomings of time taken to collect the sample, process the data, and calculate the concentrations. The National Institute for Occupational Safety and Health has developed a monitoring technique, based on filter sampling and FTIR transmission spectroscopy, for respirable crystalline silica that can provide mass concentrations by the end of the working shift, applying a software that is capable of calculating the silica mass on the filter and the silica mass concentration.

This manuscript aims to discuss the new dust generation and aerosol testing chamber developed at the University of Nevada, Reno, for dust monitoring and the evaluation of new silica dust mass concentration methods using the NIOSH FTIR standard technique. The contributions of this work include: 1) A review of RCS and coal health hazards, time integrated methods for characterization and quantification, and current silica monitoring methods. 2) The development of the aerosol testing chamber for mining environments and the application of the NIOSH FTIR standard technique. 3) Evaluation of new monitoring methods using the NIOSH FTIR standard technique. The new method is based on dust absorption spectra measurements obtained with a photoacoustic spectrometer equipped with a tunable quantum cascade laser.

Dedication

I dedicate this work to my mother, **Ailde Nogueira Lopes**, and my father, **Edson Leal do Nascimento**, who have always supported me on achieving my goals. They have dedicated their time, energy, and resources to make sure that I would have the best future I could ever dream of. They have helped me make the best decisions in life even when I was not able to see them clearly. For that, and all the love we share, I offer this manuscript, which is the materialization of one more dream, to you both.

Com todo meu amor!

Acknowledgments

Foremost, I would like to express my gratitude to my advisors **Dr. Charles Kocsis** and **Dr. Patrick Arnott** for their incessant support and assistance in accomplishing my objective of graduate education degree. They have always been patient and have motivated me to achieve the best results. Additionally, I would like to thank **Dr. Raj Kallu**, also a member of my thesis committee, for the continuing guidance throughout my academic studies.

I would like to acknowledge the **National Institute for Occupational Safety and Health** for funding the research conducted in this thesis as part of a 3-year project titled "*Development of a Personal Real-Time respirable Coal Dust and Silica Dust Monitoring Instrument Based on Photoacoustic Spectroscopy*". I also would like to thank Dr. Emanuele Cauda for his assistance and technical support with the NIOSH field based technique and the FAST software.

I would like to thank **Samuel Taylor** for being the best co-worker I could ask for; your motivation and enthusiasm helped me enjoy even more the work we did.

I would also like to thank **Annie Kocsis** for all the assistance and guidance throughout these two years. I have learned and grown a lot from working with you.

Finally, I would like to thank my dearest friends and family for all the support. I could not have gotten this far without you.

Table of Contents

List of Figures

List of Equations

1 Introduction

1.1 RCS and Coal Health Hazard in the Mining Industry

Mining is an industry that employs a considerable amount of people. Some of the mines have specific geological characteristics, which can present health and safety risks for the underground workforce, if not fully addressed. For instance, in coal, metal and nonmetal mines, miners can be exposed to elevated concentrations of respirable crystalline silica (RCS). In a mine, respirable dust is generated during the extraction by different unit operations, such as drilling, blasting, loading, and transporting. Respirable coal dust is usually a mixture of different minerals, which includes coal and silica. Silica is also present in different rocks, and is one of the most common minerals in the earth's crust, occurring naturally in the amorphous or crystalline forms (NIOSH, 2002). Silica is a mineral that is represented by the chemical compound silicon dioxide. Crystalline silica is classified as a polymorph because it can be found in more than one form. The different polymorphism of crystalline silica are alpha quartz, tridymite, beta quartz, cristobalite, coesite, keatite, stishovite, and moganite. Besides quartz, cristobalite and tridymite, the other crystalline silica polymorphs are rarely seen in nature (Ampian & Virta, 1992). Alpha quartz is the most common form of the crystalline silica, which is how RCS is sometimes designated (Schatzel, 2009). A vast number of materials contain silica in their composition and, consequently, innumerous industries have faced exposures to silica dust. Some examples of industries that have to deal with the presence of respirable crystalline silica include

agriculture, construction, manufacturing and mining (Rajavel, Raghav, Gupta, & Muralidhar, 2020).

The presence of silica in the mines is associated with a considerable number of different mineralogies. The crystalline silica can be present either in the ore rocks or in the surrounding rocks. The dangerous small particles produced in the different operations in the mine cycle can fall into the range of 0.5 to 4.0 microns. This size range characterizes the respirable dust particles, which can be easily inhaled and deposited into the lungs (MSHA, 2014). The fine particles in the respirable dust range can penetrate deeper onto the breathing system (Johann-Essex, Keles, Rezaee, Scaggs-Witte, & Sarver, 2017). The deposition of respirable dust into the structures of the lung can impact its functions as a result of damages to the alveoli, which are responsible for oxygen transfer into the body's bloodstream. Since the body is limited in means of removing such small particles from the lungs, the deposition of respirable crystalline silica and other dusts can have an extremely harmful effect on the lungs (MSHA, 2014).

The long-term exposure to respirable dust in mines, such as coal and silica, can cause occupational lung diseases that include pneumoconiosis, emphysema, and the chronic obstructive pulmonary disease, commonly known as *black lung* (NIOSH, 2002). The overexposure to respirable crystalline silica can even lead to silicosis or lung cancer (Kachuri et al., 2014). Some epidemiologic studies have shown that the risk of developing chronic silicosis is more significant when workers are exposed to respirable crystalline silica over their working life at the current permissible exposure limit (PEL) set by the

Occupational Safety and Health Administration (OSHA), the Mine Safety and Health Administration (MSHA), or the recommended exposure limit (REL) by the National Institute for Occupational Safety and Health (NIOSH). Such exposure can also be associated with the occurrence of autoimmune disorders and other harmful health effects (NIOSH, 2002). Long-term exposure to RCS and the short-term exposure to high concentrations represent a serious problem in the mine industry, which can lead to incurable diseases and even death (Laney & Weissman, 2014). This respirable health hazard can have a truly overwhelming effect upon the life of a coal worker, sometimes leading even to premature death.

1.2 Time integrated methods

Time integration methods have been extensively used to solve many types of problems. The adequate method to be applied should meet criteria, such as unconditional stability, numerical dissipation control, and low numerical effort (Bajer, 2002). Some characterization and quantification techniques that apply time integration solutions include laser induced breakdown, Raman, spark induced breakdown, X-ray diffraction and FTIR.

1.2.1 Laser induced Breakdown Spectra

Laser induced breakdown spectroscopy (LIBS) is an analytical technique considered simple and robust for quantification applications. The technique consists of using a laser pulse to strike the surface of the material. Part of the material is ablated by the laser pulse, and it is atomized. This process generates plasma containing ions and excited

atoms. Characteristic atomic and ionic emission lines can be obtained when the excited atoms and ions return to their original energy state. These emission lines can be used to characterize the composition of the material (Srungaram, Ayyalasomayajula, Yu-Yueh, & Singh, 2013). The LIBS is considered a less time-consuming technique compared to laboratory techniques such as atomic absorption spectroscopy and inductively coupled plasma-atomic emission spectroscopy because, in these methods, the samples need to be precisely prepared (Bings, Bogaerts, & Broekaert, 2010; Srungaram et al., 2013).

1.2.2 Spark Induced Breakdown Spectroscopy

Spark Induced Breakdown Spectroscopy is another quantification technique that is based on the generation of plasma. The technique consists of creating a spark between two electrodes. The spark will ablate part of the sample. The material ablated will be vaporized and will generate excited atoms. Once the atoms de-excite, the characteristic emission lines can be detected and the composition of the sample can be determined (Srungaram et al., 2013). Some advantages of the SIBS compared to the LIBS are the more compact sizes that it can be configured and manufactured and the cost-effectiveness. Additionally, SIPS can be used in analysis of gaseous dispersions when the breakdown voltage of the medium is low (Jung, Yang, & Yoh, 2020).

1.2.3 Xray diffraction XRD

X-ray diffraction (XRD) is a widely used technique applied to the characterization of crystal, and it is a technique based on the interference of monochromatic X-rays and the

crystalline sample material being used. The technique consists of generating X-rays using a cathode ray tube and filtering it to create the monochromatic radiation, which is later collimated in order to concentrate. The radiation is then sent toward the sample material. Once the incident ray interacts with the crystalline sample, constructive interference and a diffracted ray are produced when the geometry of the X-ray intruding the material meets Bragg's Law. The diffracted X-ray can be counted after being detected and processed. Bragg's Law relates the wavelength of the X-ray (lambda) to the inter-planar spacing (d) that generates the diffraction and the angle of diffraction (theta). Each crystalline material has a set of unique interplanar spacing, which allows the identification of the compound by converting the diffraction peaks into d-spacing. The X-ray diffraction is a non-destructive technique that can be used for identification of minerals swiftly, but it requires a standard reference database in order to identify the crystalline samples (Bunaciu, Udristioiu, & Aboul-Enein, 2015). Additionally, the XRD technique requires adequate sample preparation for analyzing powder samples, which should be in the size range of 1-5 microns (Cullity, 1978).

1.2.4 Raman

Raman spectroscopy is a vibrational spectroscopy technique used to study a vast number of sample types. Raman can be used to identify samples in simple or complex ways, which may include a full spectrum for qualitative and quantitative analysis. Raman spectroscopy occurs based on the off-resonance interaction of radiation with molecular vibrations, which considers the Raman polarizability of the matter, and it is mostly applied for

symmetric vibrations of non-polar groups. The vibrational bands are determined by the frequency, intensity, and band's shape (Larkin, 2011). The technique is based on Raman scattering, a process that involves photons that are shifted in frequency when losing or gaining energy, according to the energy of the specific vibrational transition (Agarwal & Atalla, 1995). Shifts in the energy are used to gather information regarding the composition of the molecules in the sample (Shipp, Sinjab, & Notingher, 2017). The Raman spectroscopy process consists of monochromatic irradiation of a sample by a laser, which generates Raman bands when the molecular vibration changes the polarizability. In the Raman phenomena, the scattered photon is a result of the transition from the virtual state to the excited state of the molecular vibration, which is an inelastic collision, resulting in a photon with different frequency (Larkin, 2011). The Raman technique for inquiring spectra can be considered a non-destructive technique and can be performed using visible wavelengths (Shipp et al., 2017). One disadvantage of Raman spectroscopy is the presence of weak signals, which can cause an increase in the acquisition time. This shortcoming can be addressed by applying coherent Raman techniques, such as the Coherent anti-Stokes Raman Scattering (CARS) or the Stimulated Raman Scattering (SRS) (Evans & Xie, 2008).

1.2.5 Fourier Transform Infrared Spectroscopy (FTIR)

When electromagnetic radiation is directed to a substance and they interact, it results in reflection, absorption, transmittance, or scattering of the radiation. These processes can be used to collect important information about the molecular structure of the substance

and its energy level (Abu Bakar, Cui, Abu-Siada, Li, & Ieee, 2016). Infrared spectroscopy consists of the study of the interaction of electromagnetic radiation with molecular vibrations. In the infrared spectroscopy technique, the transitions between vibrational energy levels of the molecules are measured because of the absorptance of infrared radiation. The interaction present in the infrared spectroscopy is a resonance condition that involves electric dipole change between vibrational energy levels (Larkin, 2011). Based on the fundamental vibrations of a functional group, typical infrared absorptance bands can be identified (Griffith & de Haseth, 1986). A normal mode of a molecule is related to the vibrational motions of the atoms. In the case of a nonlinear molecule containing A atoms, 3A-6 normal modes exist. When there are changes in the dipole moment of the molecule, a normal mode of vibration is classified as infrared active. On the other hand, when there is no change in the dipole, the vibration is infrared inactive (Berthomieu & Hienerwadel, 2009).

During the infrared absorption process, energy is absorbed by the molecules if the vibration produces a shift in the dipole moment, which will cause a change in the vibrational level. Vibrations that are asymmetric or out of phase, as well as polar groups, are generally easier to be studied by infrared spectroscopy. Classifying molecules by their symmetry is important to allow comprehension of how the structure of the molecule is related to the vibrational spectrum. Some examples of symmetry elements are axes of symmetry, center of symmetry, and planes of symmetry (Larkin, 2011).

The intensity of the absorbed and transmitted infrared radiation and the analyte concentration is overseen by the Beer-Lambert law. Spectra are generated by plotting the absorption or transmission against the wavenumber. The wavenumber is proportional to the energy difference between the different vibrational states (excited and base) (Larkin, 2011). FTIR spectroscopy can be applied in a large range of sample identifications (Berthomieu & Hienerwadel, 2009). When samples on a filter are placed in the way of the infrared beam, the sample will absorb and transmit light. The light signal is collected then at a detector, which will measure the light intensity being absorbed by the sample and the intensity being transmitted through the sample. The FTIR instrument has an output as a function of time, which is displayed as a plot of absorption or transmittance and wavenumber by using a Fourier transform technique (Abu Bakar et al., 2016).

1.3 Standard Silica Monitoring Techniques

Diseases caused by exposure to Respirable Crystalline Silica can be avoided when engineered techniques to decrease the concentration of respirable particles in the air are applied (Colinet, Listak, Organiscak, Rider, & Wolfe, 2010). Nevertheless, the constant exposure monitoring of respirable crystalline silica is essential to certify the efficacy of such control systems (Pampena, Cauda, Chubb, & Meadows, 2020). Several monitoring methods to measure the mass concentration of RCS have been applied in different mine environments and operations in order to reduce the exposure of workers to high concentrations. The monitoring methods vary according to the sampling methodology, or the analysis applied to the samples collected. For instance, some of these techniques

include the collection of samples on filters, following laboratory analysis and calculation of mass concentration. These techniques can require sample treatments and redeposition on new filters before the material is analyzed (Hart et al., 2018). Some standard silica monitoring methods include the NIOSH 7500, NIOSH 7603 and the MSHA P7 (MSHA, 2013; NIOSH, 2003a, 2003b).

One of the major disadvantages of these methods is the time required for the samples to be analyzed and for the calculation of mass concentrations. This shortcoming is a result of sample preparation (ashing or dissolving the samples). In some cases, it may take days or weeks to get analysis results. As a result, interventions are taken in an ineffective and inopportune way (Pampena et al., 2020). Aiming to overcome such disadvantages, nondestructive and more effective methods can be applied. For example, recently, a field-based technique has been developed by NIOSH, which allows the measurement of respirable silica concentrations in a more time-effective way. The technique has shortened the time delay for getting the results, which now can be obtained at the end of the shift (Pampena et al., 2020).

1.3.1 MSHA P7

A commonly used laboratory method for identifying the silica concentration in respirable dust is the MSHA P7. This is a technique developed by the Mine Safety and Health Administration (MSHA) and is based on the infrared determination of silica in respirable coal mine dust. The spectra is generated using a Fourier Transform infrared spectrometer

(PE Model 2000, GX or any equivalent). The sampling process starts with the pre-weighing of membrane filters and the collection of airborne respirable dust using personal respirable dust samplers approved by MSHA or NIOSH. The sampler apparatus consists of 37mm cassettes, PVC filters, and respirable coal dust samplers at 2.0 liter per minute airflow. Once the filters are loaded, they are reweighed using a scale to the one thousandth of a milligram precision. The reweighing of the exposed filters will provide the net sample mass. The sample filters are then ashed in order to eliminate the presence of organic matter, which are the coal dust and filter media. This step is carried out using a low-temperature radio frequency asher. After the organic matrix is removed, the sample is redeposited onto a vinyl acrylic copolymer, VAC (DM450) filter, onto a 9 mm diameter area. The redeposited sample is then scanned using infrared spectroscopy at a wavenumber range of 1,000 to 700 cm^{-1}. This wavenumber range will allow the determination of quartz and kaolinite content in the sample. The characteristic absorbance peak area for quartz is within the range of 815 to 770 cm^{-1}. However, kaolinite absorbance is also present in the same region, interfering in the quartz determination. In order to remove the interference of kaolinite, the content of kaolinite is determined at its most characteristic peak area (930 to 900 cm^{-1}), and its content is calculated. Once the kaolinite is determined, the mass of the quartz is determined by correcting for the kaolinite interference. It is fundamental that the kaolinite interference be corrected in order to avoid the overestimation of quartz mass (MSHA, 2013).

In the MSHA P7 method, the determination of quartz is carried out by comparison to calibration curves for standard quartz and kaolinite samples, which are meticulously prepared and have different load masses. For kaolinite, once the calibration samples are prepared, they are scanned in the FTIR in the range of 1,000 to 700 cm^{-1}. A calibration program is then used to determine the calibration factor, which is the slope of the line generated when calculating the least squares fit, zero intercept linear regression from peak area 915 to 800 cm^{-1}. This calibration factor will be used to determine the influence of kaolinite in the characteristic quartz peak area. A second factor will be determined by performing a least squares fit, zero intercept linear regression on 915 cm^{-1} peak area to attain the mass of kaolinite. For quartz, once the calibration samples are prepared, they will be scanned for the absorbance peak area at 800 cm^{-1} maximum. Applying the calibration program, a calibration factor can be determined by performing a least squares fit, zero intercept linear regression on the absorbance peak area at 800 cm^{-1} to the quartz mass of the samples. This calibration factor will be used to calculate the mass of quartz in the sample, which corrects for the kaolinite interference (MSHA, 2013).

The kaolinite contribution to the quartz peak area can be determined by dividing the kaolinite absorbance at 915 cm^{-1} peak area by the calibration factor calculated for kaolinite. After subtracting the kaolinite interference at the quartz peak area from the absorbance peak area at 800 cm^{-1} that accounts for quartz and kaolinite, the corrected absorbance peak area for quartz will be determined. Finally, the mass of quartz can be determined by dividing the corrected peak area for quartz at 800 cm^{-1} by the calibration

factor for quartz. The percentage of quartz in the sample can be found by dividing the mass of quartz calculated by the mass of sample (MSHA, 2013).

1.3.2 NIOSH methods (0600, 7500, 7603)

The National Institute of Occupational Safety and Health has issued several methods for monitoring respirable particulates and, specifically, silica dust. The NIOSH 0600 method is a technique for respirable particulates not otherwise regulated. The method applies a gravimetric procedure to measure the dust concentration of PM4 aerosol collected on filters. The method has been recommended for respirable coal dust. The sampling process consists of using a cyclone sampler connected to a personal sampling pump that operates from at 1.7, 2.2, or 2.5 liters per minute, depending on the cyclone used. The sampler collects dust on filters made of polyvinyl chloride or any equivalent hydrophobic membrane and is supported by a cassette. Before sampling, the filters are equilibrated for at least 2 hours and are posteriorly pre-weighed for relative humidity control. The filters are then placed into the cassette and connected to the sampler system. The samples are collected during a range of 45 minutes to 8 hours, avoiding overloading the filters with more than 2 mg of dust on the filters. After being loaded, the filters are then equilibrated again for at least 2 hours in a controlled area before they are weighed. The post weights are then recorded, and the determination of dust concentration can be made. The concentration of respirable particulate (mg/m3) can be determined by the following equation, which takes into account the mean tare weight of a blank filter (B1) in mg, mean tare weight of a loaded filter (B2) in mg, filter weight before sampling (W1)

in mg, filter weight after sampling (W2) in mg, and the volume sampled at nominal flow rate (V) in L/min (NIOSH, 1998).

$$C = \frac{(W2-W1)-(B2-B1)}{V} * 10^3 \qquad \textit{Equation 1}$$

Another NIOSH technique for dust monitoring is the NIOSH 7500, which is a method applied specifically for crystalline silica determination by using X-ray powder diffraction. This is a destructive technique that uses filter preparation and re-deposition of the sample for analysis. The equipment used consists of a cyclone sampler, sampling pumps with flexible connecting tubes, 37 mm PVC filters, and cassette filter holders for sampling. The sample will be re-deposited onto silver membrane filters of 25 mm diameter. An X-ray powder diffractometer, which is equipped with a copper target X-ray tube, graphite monochromator, and scintillation detector is used to identify the crystalline silica on the re-deposited sample after it is ashed by a low temperature radio-frequency plasma asher. A muffle furnace or an ultrasonic bath can also be applied for filter preparation (NIOSH, 2003a).

In the NIOSH 7500 technique, the personal sampling pumps need to be calibrated. The total sample size or sample volume should be between 400 to 1000 L for a pump flow rate or 1.7 or 2.2 liters per minute when using a nylon cyclone or a HD cyclone, respectively. It is fundamental to take precaution and do not invert the sampler assembly at any time in order to avoid the oversized material to be deposited onto the filters. Once the samples are collected onto the filters, they need to go through a preparation process that results

in the destruction of the filters and re-deposition of the samples onto new filters. The samples are prepared by applying a low temperature ashing technique, or a muffle furnace ashing, or a filter dissolution technique. A silver filter is then prepared for redepositing the sample. Once the sample is redeposited onto the filter and it is ready for measurements, the silver filter is placed in the XRD sample holder. A qualitative X-ray diffraction scan is generated in order to define the occurrence of silica polymorphs and interferences. Quartz has its primary, secondary, and tertiary peak with 2 theta degrees at 26.66, 20.85, and 50.16 respectively (NIOSH, 2003a). The first step in performing the XRD measurements, when using the NIOSH 7500 method, is mounting the reference specimen, which can be mica or other stable standard that can be used for data normalization, and determining the net intensity of the reference specimen I_r. The sample is mounted, and the diffraction peak area for the silica polymorph is measured. The background is measured on each side of the peak, and an average background is calculated by averaging the two measurements. After, the net intensity I_x is calculated, which is the difference between the peak area count and the total background count. The normalized intensity $\hat{I}_x$ can then be determined for each peak by dividing the net intensity I_x by the net intensity of the reference specimen I_r, times a normalization factor N (equivalent to the reference specimen net count). Once the normalized intensity is calculated, the concentration of crystalline silica (C) in mg/m^3 can be determined using the following formula, which takes into account the normalized intensity for sample peak ($\hat{I}_x$), the intercept of calibration graph (b), the slope of calibration graph in counts/ug (m)

and the function f(t), which is the absorption correction factor, and the air volume sampled (V) in L (NIOSH, 2003a).

$$C = \frac{\hat{I}x * f(t) - b}{m * V}$$ *Equation 2*

Another NIOSH method used for silica determination is the 7603 technique for silica determination in coal mine dust is also a destructive method that uses re-deposition of the sample. Differently of the NIOSH 7500, the 7603 method applies infrared absorption spectrometry in order to determine the concentration of silica in the sample. The sampling apparatus used is similar to the one applied in the NIOSH 7500 method. A 10 mm nylon or a HD cyclone is used with sampling pumps connected. The 37 mm filter is placed into a two-piece filter cassette holder. A head holder is used in order to keep the apparatus held together. The filters are pre-weighed before sampling starts to the nearest 0.01 mg. The samples are taking in a total volume sampled of 300 to 1000 liters, and it is important to make sure that the total loaded sample is not greater than 2mg. At any time during the sampling, the apparatus should not be inverted. Otherwise, the oversized particles collected in the grit pot of the cyclone will be deposited onto the filters. The sample preparation process consists of reweighing the filters after they have been exposed, making sure that the ambient conditions are similar to the ones when the pre-weights were taken. The difference between the post exposure filter weight and the pre-exposure filter weight is the sample weight. The samples can be ashed by a low temperature ashing process or a muffle furnace ashing. Once the sample is ashed, it is redeposited onto a new filter using a filtration apparatus (NIOSH, 2003b). The redeposited

sample will be used in an infrared spectrometer through a scan range of 1000 to 650 cm^{-1}. The presence of quartz is determined by the peak area of 820 to 670 cm^{-1}. In case there is kaolinite present, a band will be seen between 960 and 860 cm^{-1}, and the interference of kaolinite at the quartz characteristic peak area needs to be corrected. The interference of kaolinite can be corrected by deducting the absorbance of kaolinite at the 915 cm^{-1} peak from the 800 cm^{-1} peak. The quartz weight is determined after correction for kaolinite interference, in case it is present, by using the absorbance at 800 cm^{-1}. The weight of quartz is determined from standard curves. Finally, the percentage of quartz in the sample will be determined by dividing the quartz weight by the sample weight (NIOSH, 2003b).

1.3.3 Quantum cascade laser (QCL) based on infrared absorption spectroscopy

An alternative technique for identifying the RCS concentration of aerosol consists of applying a tunable quantum cascade laser (QCL) based on infrared absorption spectroscopy. The sampling method is similar to the ones applied in the standard techniques and also involves the treatment of the sample collected and re-deposition of the material on a new filter prior to the analysis. The quantification of alpha quartz is obtained through analysis of infrared transmission measurements employing the QCL and a mercury-cadmium-telluride detector (Wei, Kulkarni, Zheng, & Ashley, 2020).

1.3.4 NIOSH Field-based silica monitoring method and FAST software

A recent crystalline silica monitoring technique has been developed by NIOSH, which allows for a silica mass concentration determination at the end of a shift. Compared to the other monitoring methods by NIOSH and MSHA, the field-based silica monitoring method eliminates the long wait time for getting the silica concentration data – usually one to two weeks because of the sample preparation and laboratory work. The sampling system is similar to the MSHA P7 method and consists of a personal sampling pump that is connected to a PM4 cyclone. The system apparatus contains a cassette with a filter, onto which the sample is collected throughout the shift. The loaded filters are collected at the end of the shift, and a portable Fourier-Transform Infrared Spectrometer (FTIR) capable of generating spectra over a range of 4000-400 cm^{-1} at a resolution of 4 cm^{-1} is used in order to analyze the samples. The measurements start by generating a background spectrum using a clean, unexposed filter from the same filter batch used for collecting samples. This background transmittance is removed from the spectra generated using sampled filters (Pampena et al., 2020).

The determination of respirable crystalline silica concentration during the shift is proceeded by using the NIOSH software known as Field Analysis of Silica Tool (FAST). The software is capable of receiving data from a FTIR spectroscopy instrument and converting it into a silica mass and silica concentration per respirable dust sample, based on the values of sampling time and pump flow rate (Pampena et al., 2020). After the spectra are generated in the FTIR instrument, they must be analyzed by the instrument in order to

generate the integration of silica and other minerals. Currently, the NIOSH FAST supports importing data from four different instruments: Argilent, Bruker, Perkin Elmer and ThermoFisher. After generating the spectra and carrying out the analysis of the samples, these instruments can export .CSV or .XLS files that can be imported into and read by FAST. It is also possible to create a generic .CSV, when another FTIR instrument is used, and import it into NIOSH FAST – the file needs to contain the mandatory fields: sample name, M, D, C, Q, and K. The last five fields are integration areas of absorbance spectrum of a single sample. The variables represent different minerals with their signature features in the spectrum. Q is the signature feature for quartz, K represents kaolinite, M represents microcline, C is related to calcite and D to dolomite. However, at the moment, FAST only uses the values of quartz and kaolinite from the integration of specific areas in the spectrum. The other variables are collected for potential future use. NIOSH has available macros for each FTIR unit that have been tested, which may be used to perform the integrations (NIOSH, 2020).

When the data is imported into FAST and the event for the samples is created, it is necessary to choose the commodity that best represents the mine's production. The software will use this information to determine the RCS based on the mine's mineralogy. As mentioned, each value of the variables generated in the FTIR analysis will represent the presence of different minerals that may impact the concentration of silica in the sample. However, FAST is currently only capable of accounting for mineral interference from samples collected in coal mines, for there is a quantification model that has been

developed taking into consideration the minerals associated to the commodity (coal). The silica mass and concentration in samples collected for any other commodity will be calculated as an estimation of the RCS in the sample, based only on the variable Q. A correction factor can be obtained by doing a linear regression of the values of silica mass calculated in FAST and the laboratory silica mass obtained from standards methods applied on the same filters by an external laboratory. Once the correction factor is obtained, it can be applied for silica calculations from samples collected at the same worksite in order to generate more accurate results for silica mass and concentration (NIOSH, 2020).

Some difficulties can be faced when using the field-based NIOSH technique, such as the complexity of defining a quantification model for worksites other than coal mines or defining a correction factor. However, the field-based method is an improvement when compared to previous methods applied for RCS concentration determination (S.J. Taylor, To Be Published).

2 Methods

2.1 Development of an Aerosol Testing Chamber for Mining Environments

The application and evaluation of dust monitoring techniques needed to be carried out with conditions that fairly represented the mine environments – mainly the underground environments. The need to generate dust in suspension that could emulate ambient conditions in working areas in a mine was met by developing an aerosol testing chamber

that was capable of providing uniform concentrations in the testing section and stable dust plumes. Although the dust testing chamber presents several particularities, it was based on the standard aerosol testing chamber (e.g. Marple-type) developed by NIOSH.

NIOSH has developed an aerosol chamber in order to carry out evaluation and calibration of many measuring instruments and samplers. This chamber, also known as Marple Chamber, has the capability of evaluating different instruments at the same time, allowing the instrumentation to be also placed inside the chamber during the tests. Placing the instruments inside the chamber is important to account for interference of the instrument's heat sources, for instance. The chamber is equipped with a rotating table that allows the samplers to collect from different regions in the chamber. However, it has been shown that the concentration is uniform in the testing section. Additionally, the testing chamber has shown good temporal stability of the dust plume (Marple & Rubow, 1983).

The UNR aerosol testing chamber can be considered a "Marple-type" chamber, for it allows the use of many instruments, both inside and outside the chamber, at the same time and also presents a uniform concentration in the test section and a stable plume that decays slowly with time. The chamber was constructed from industrial grade 1/8-inch steel plates and a Plexiglas plate, both heavily insulated at the edges. The chamber is 1.66 m high, 0.81 m deep and 1.97 m wide, which accounts to a total volume of 2.65 m^3. The dust chamber is located at the ventilation laboratory at the University of Nevada

Reno and was initially built to evaluate control of ionizing radiation by using HEPA type filters.

The testing chamber was redesigned for dust monitoring and simulation of the mining environment, allowing measurements of a vast number of aerosols, mainly mineral dust that is generated during production activities in underground mines. Some of the aerosol tested in the dust chamber includes silica, kaolinite, coal, graphite, and incense. However, the focus has been on the monitoring of silica, kaolinite, and coal dusts. Some changes made in the chamber consisted of removing the HEPA type filters compartment. This step was important to allow recirculation of the aerosol, in case it was needed, without having the particles be captured by the HEPA filters. A window was placed on the chamber in order to allow access to its interior, which was crucial for more time efficient preparation of experiments. Additionally, several through fitting connectors were installed in the Plexiglas, which allows the use of several instruments at the same time during an experiment. The chamber piping system was redesigned with the placement of dampers that allows the insulation of the chamber and also helps with the complete removal of the aerosol from inside the chamber when the experiments are done. All the connections in the chamber and in its piping system were sealed. The chamber is well sealed in order to avoid leakage of aerosol into the room. Finally, a fume hood is connected to the piping system, which also helps with the complete exhausting of the aerosol plume inside the chamber at the end of experimentation.

Even though the dust testing chamber has been well sealed, and the system is considered very safe, additional health control means are taken throughout the experiments. Firstly, the access to the dust room is limited to the personnel involved in the experiments and everyone is required to comply with the safety measurements. Everyone who is present in the dust room during an experiment is required to wear N95 masks or respirators. A dust mass concentration instrument is used inside the dust room at any time during an experiment. The measurement of dust concentration in the room is carried out by a DustTrak instrument (Model 8520, S/N 85200408, from TSI), and any experiment needs to be immediately interrupted when the concentration in the room is above the permissible limits of exposure. The placement of the comminuted mineral in the bowl for dust generation needs to be performed inside the chamber, avoiding the deposition of mineral particulates outside the testing chamber. Before generating the dust plume, the whole system needs to be checked, making sure that the dampers are closed and that the window door in the chamber is sealed. Finally, after the experiment starts, the dust chamber can only be cleared after the exhausting system is activated and the concentration inside the chamber is considered safe.

In order to control, maintain and clear the suspended aerosol inside the chamber, there is a PVC piping system equipped with regulators and dampers, and is connected to a centrifugal fan (S/N 91-86972-1-1 from Twin City Fan & Blower CO.) that provides the required pressure to generate airflow in the system. The aerosol delivery system consists of a metal bowl containing the material to be dispersed and a compressed air unit. The

compressed air unit is connected to a tube, which is placed inside the dust chamber through one of the feed-through connectors on the Plexiglas, and it is directed to the bowl inside the chamber that contains the powder to be suspended. The bowl is loaded with the comminuted mineral used to generate the aerosol plume. Once the system is ready for the experiment, which includes the monitoring of the dust concentration in the room and the use of Personal Protective Equipment (PPE), the compressed air system is fired by opening the unit's valve and letting it hit the bowl for approximately 5 seconds before the valve is closed. Other through fitting connectors allow the installation of the photoacoustic instrument, a cyclone sampler in order to reproduce the NIOSH standard technique, as well as other sampling methods' instrumentation such as the APS and ELPI instruments. Additional to those instruments, a SPS30, which is a low cost air quality sensor based on aerosol light scattering, is installed inside the chamber and its data is transmitted through a cable to a computer in the room, allowing the monitoring of the concentration and size distribution of the aerosol inside the chamber.

The UNR dust chamber has been used in the generation of different types of aerosols (silica, kaolinite, graphite, coal, and mixtures of silica/coal and silica/kaolinite) that slowly decay over approximately 2 hours and stabilizes approximately 6 minutes after the dust is generated, which allows the collection of samples over a long period of time by different sampling methods that can be used simultaneously. Once the sampling is finalized for each experiment, the ventilation system equipped to the chamber is initiated. This system clears the chamber using the fan and the piping system and allows the removal of the

dust after approximately 4 minutes. The ventilation system is turned off, and the chamber is considered safe to be open after the concentration in its interior reaches 20 $\mu g/m^3$. Figure 1 shows the UNR Marple type chamber , which is the device with the window attached, the Fume Hood, the Dustrak and Photoacoustic Instruments, and the Exhausting System (fan and pipes). The SPS30 and the cyclone sampler are placed inside the chamber. As mentioned, the dust testing chamber is capable of simulating mining environment conditions, by generating dust in suspension. The evacuation system, which consists of several pipes, valves, and dampers connected to a centrifugal fan, also allows the recirculation of dust in the chamber, in case it is needed. The recirculation of aerosol in the dust chamber can represent mine conditions where the recirculation of dust occurs.

Figure 1: Marple-type dust chamber setup.

2.2 Photoacoustic Instrument

The need for applying a real time dust monitoring technique is the major goal of the research funded by NIOSH. The project's aim is the development of a real time dust monitoring instrument based on photoacoustic spectroscopy. The principle of the instrument is light absorption (S. J. Taylor, Nascimento, Arnott, & Kocsis, To Be Published). The aerosol inside the chamber is pulled through a resonator by a vacuum pump. At this point, a quantum cascade laser (QCL), which is power modulated, sends a laser beam that enters the window on the left side of the resonator chamber. As the light interacts with the aerosol in the resonator chamber, part of the light is absorbed and heats up the particles in the chamber. The energy absorbed by the particles is then transferred to the surrounding air, and a specific sound is generated due to the expansion and contraction of the air. The sound generated is measured and recorded by a highly sensitive microphone. The laser light that is not scattered or absorbed is capture by an integrating sphere and measured by a mercury-cadmium-telluride (MCT) detector. The QCL is set to the same modulation frequency of the resonator chamber (Arnott, Hamasha, Moosmuller, Sheridan, & Ogren, 2005). The dust absorption coefficient is calculated using the sound pressure P_m, laser power P_L, resonator cross sectional area A_{res}, ratio of specific heats γ for air, resonator quality factor Q, and resonance frequency f_0 (Arnott, Moosmuller, Rogers, Jin, & Bruch, 1999).

$$B_{abs} = \frac{P_m}{P_L}\frac{A_{res}}{\gamma - 1}\frac{\pi^2 f_0}{Q} \qquad \textit{Equation 3}$$

Figure 2 shows the photoacoustic diagram for the instrument used in the experiments. The results obtained by the photoacoustic will be compared to the SPS30 and the NIOSH standard technique.

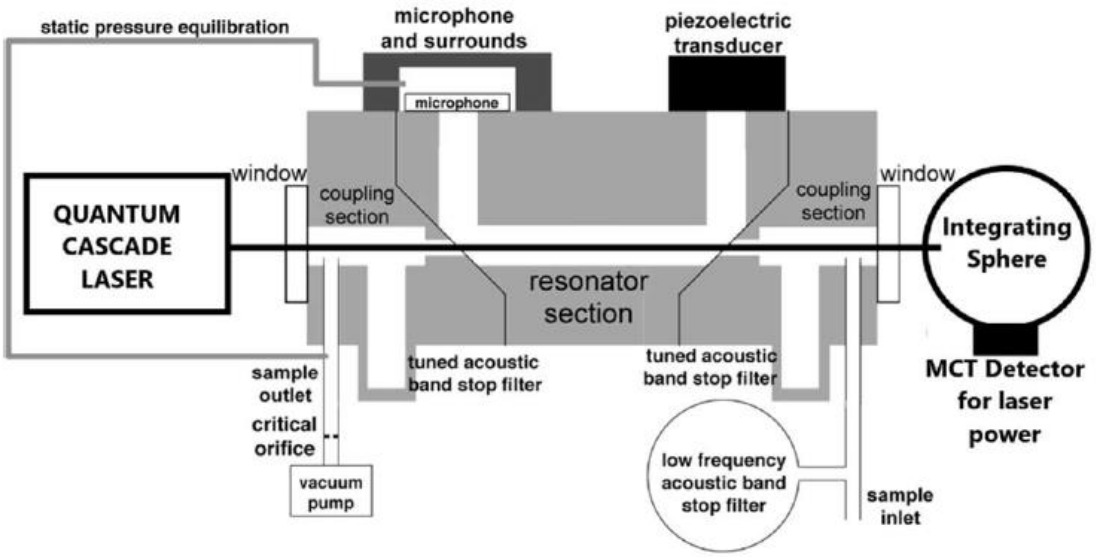

Figure 2: Diagram of the photoacoustic instrument.

2.3 APS and SPS30 Instruments

In order to validate the use of the SPS30 as the mass concentration monitoring instrument used in the experiments, aiming for both safety and to confirm the results of mass concentration obtained by the NIOSH technique and the photoacoustic instrument, the TSI Aerodynamic Particle Sizer (APS) was applied in some experiments. The APS is a well-known and used instrument for mass concentration monitoring. The Sensirion SPS30 is a compact and low-cost air quality sensor (Nascimento et al., 2021). The results obtained with the SPS30 and the APS were compared and will be presented in this manuscript.

2.4 NIOSH FTIR Filter-based Silica Monitoring Technique and FAST Software

2.4.1 Sampling

The filter sampling method aims to reproduce the Field-Based Silica Monitoring Technique developed by NIOSH, which is applied for measuring silica concentration at the end of the shift in coal mines. At the ventilation laboratory at UNR, filters are loaded with the samples and are posteriorly used in a FTIR instrument at the Chemistry department in order to generate the transmission spectra to be used for the silica mass concentration calculations. As mentioned, the ”Marple-type” chamber at UNR is used to generate the dust plume, and, through one of the feed-through connectors, a cyclone sampler is used to load the filters. The sampler arrangement consists of an “SKC-type” aluminum cyclone (Zefon International, Catalog NO. ZA0060), cassettes (Zefon International, REF 745PVC-CF-FTIR), 37 mm PVC filters (Zefon International, REF FSP37R), and tubing connected to a pump (Zefon International, N 629946).

Once the material is placed inside the chamber, a blank filter, which is already labeled and had its reference transmission spectrum generated, is placed in the cassette. The sampling apparatus (cassette and cyclone) is then assembled, and the outlet of the system is connected to the pump by tubing. The pump is calibrated two times before the experiment. First, the pump flow is calibrated to 2.5 LPM using a flow meter instrument (QPS, Inc. S/N 162390) without connecting it to the tubing. Once the pump flow is achieved, the pump is connected to the tubing, and it is calibrated again in order to account for the pressure loss of the tubing arrangement. Having calibrated the pump, the

sampler system is mounted inside the chamber. Before each new experiment, the pump is calibrated again to assure that the adequate flow rate is being used. Figure 3 shows the sampler arrangement used for collecting samples onto the filter.

Figure 3: Cyclone sampler arrangement.

The cyclone sampler operates at a sampling flow rate of 2.5 LPM for a 4-um cut-point. The cyclone used is a perfect replica of the SKC aluminum cyclone, which is specified in the NIOSH 7500 method for silica and NIOSH 0600 method for respirable particulates (NIOSH, 1998, 2003a). The Aluminum Cyclone is a lightweight respirable particles sampler that when connected to a sampling pump, respirable dust particles are collected onto the filter and particles above the cut-point are captured into the grit pot and are later discarded, providing a considerable size selection of the PM4 fraction. The separation efficiency curve conforms to the standards defined by ACGIH/ISO/CEN for a respirable curve with a d50 cut point of 4 microns at a flow rate of 2.5 LPM (OSHA, 2013).

Figure 4 and figure 5 present the curve efficiency in conformance with the ISO7708/CEN criteria and the d50 of 4 um for 2.5 LPM for the SKC aluminum cyclone (SKC, 2021).

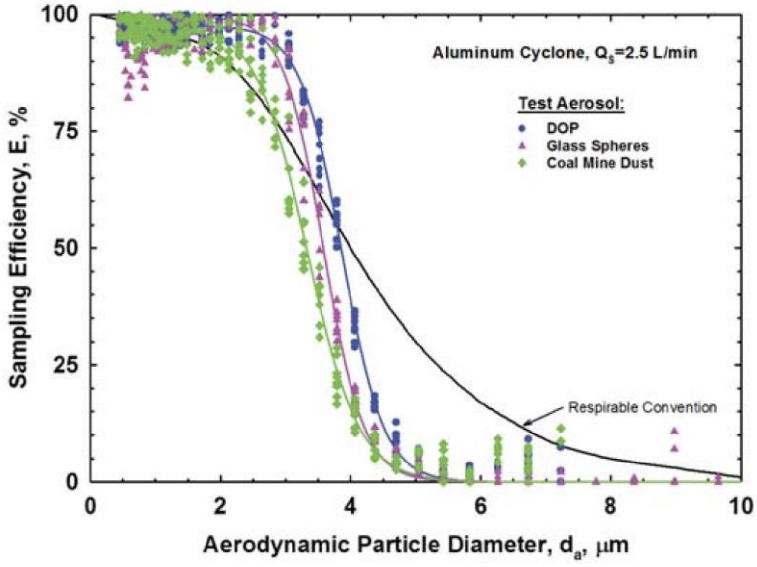

Figure 4: Collection efficiency relative to ISO 7708/CEN criteria in OSHA silica rule and ACGIH TLVs (SKC Manual, 2021).

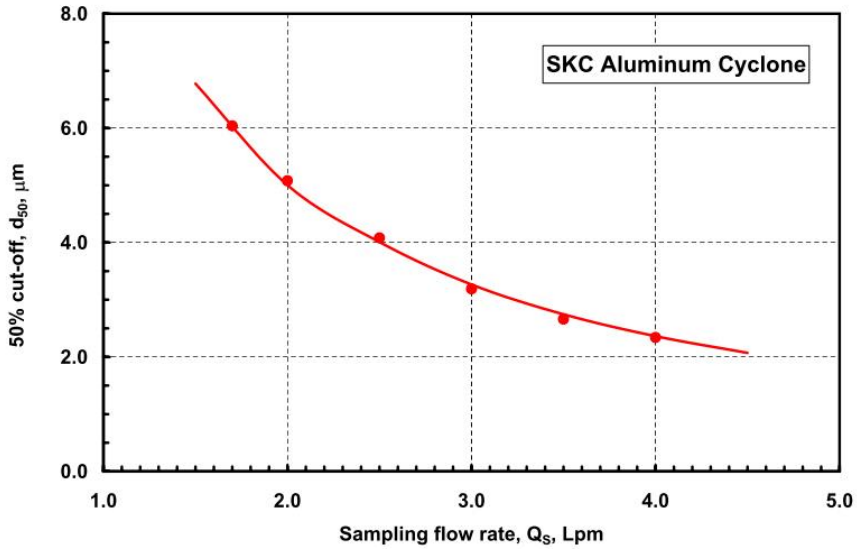

Figure 5: SKC Aluminum cyclone cut-off flow rate (SKC Manual, 2021).

Once the dust cloud is produced, the pump is turned on after the plume decay curve, generated by the SPS30 instrument, has stabilized. In general, it takes around 6 minutes for the decay curve to be stable, and it slowly decays with time. The sampling duration time has varied from 2 to 3 minutes. This sampling duration time range has been experimentally chosen as the best, for the results obtained are satisfactory. It allows the filters to be loaded with enough mass to be above the limit of detection (LOD) and limit of quantification (LOQ) established in the NIOSH FAST software. The LOD and the LOQ are based on the Q value, which is the area under the curve of the characteristic peak for silica (the peak area with strongest absorption). Any sample which has a Q value imported from the FTIR instrument lower than 0.026 cm^{-1} falls into the LOD classification. The limit of quantification is any sample which has a Q value imported from the FTIR instrument greater than or equal to 0.026 cm^{-1} and lower than 0.078 cm^{-1}. According to the NIOSH FAST Manual, when the Q input values fall below or within a specific range, the results are not reliable due to the calculations applied for silica mass concentration (NIOSH, 2020).

After having a stable decay curve for the dust plume, the pump is turned on and the sampling starts. The pump is turned off after the sampling duration is completed. The sample volume can be determined by multiplying the flow rate, measured during calibration, by the sampling duration. The cyclone is only removed after the chamber is cleared and is considered safe to be opened. At this point, the window is opened, and the cyclone sampler is removed. The cassette is carefully opened, and the filter is removed

and placed into a filter holder for posterior FTIR measurements. This step is carefully carried out, making sure that the cassette is not flipped, and the oversized particles are not deposited onto the filter. Additionally, the filter is cautiously removed in order to avoid any damage to the filter media structure.

The area of the filter that is loaded with the sample has been estimated based on the area of the filter that is exposed to the flow. The filter is held in the cassette by a metal ring, which allows the filter to stay still and not be suctioned by the negative pressure in the outlet of the cassette. As a result, there is a reduction of the filter area exposed to sample deposition due to the metal ring blocking the airflow. Figure 6 shows the area of the filter that is exposed and the metal ring used to support the filter in the cassette. Based on the filter diameter and on the dimensions of the metal ring, the area of the filter that is exposed to the dust collection was estimated as 6.92 cm^2. The ring dimensions were measured using a caliper.

Figure 6: Metal ring and blank filter before sampling.

Determining the area of the filter that is exposed to the sample collection is crucial for calculating the absorption coefficient for the sample collected on the filter. This calculation is carried out after the normalized transmission is obtained.

Figure 7 shows some loaded filters that were obtained from experiments in the aerosol testing chamber and a blank filter used as reference for background removal in the FTIR.

Figure 7: Blank filter and loaded filters obtained from experiments in the aerosol testing chamber.

2.4.2 FTIR Spectroscopy

The exposed filters are taken to the Chemistry department and are used in the FTIR instrument (NICOLET 380 FT-IR, by ThermoFisher) for spectra generation. The FTIR does a spectroscopic transmittance measurement of aerosol deposited on the filter for a given wavenumber range. The transmission spectra are then converted into absorbance to

obtain mass concentration of a mineral, based on its characteristic absorption peak area in the spectrum. In order to get transmission measurements on the filters, a filter holder for placing the filters in the FTIR instrument was created. The filter holder was filed to fit the metal holder inside the ThermoFisher FTIR. The holder had a hole drilled in its center to allow the FTIR beam to penetrate only the filter, avoiding interference from the filter holder structure. Figure 8 shows one of the filter holders used during the FTIR measurements.

Figure 8 Filter holder used in the FTIR instrument.

The FTIR instrument is prepared for the measurements by setting it to transmittance mode and turning the purging system on. The purging of the instrument allows the removal of water vapor and CO_2 interference in the spectrum. In addition to the purging setup, an automatic alignment is initiated in order to guarantee a good performance of

the instrument. The transmission measurements are taken over a spectral range of 4000–400 cm^{-1} at a resolution of 4 cm^{-1}. The transmission spectrum is obtained based on an average of 32 readings. Before the first measurement, the FTIR chamber is purged for approximately 10 minutes. After the first purging, every time that the chamber is open, it needs to be purged again for 2 minutes before the FTIR transmission measurement is taken. Figure 9 shows the FTIR instrument setup used for the transmission spectra taken during the experiments.

Figure 9 FTIR instrument (NICOLET 380 FT-IR, by ThermoFisher).

2.4.3 Transmission Spectra Normalization

When generating the transmission spectra using filters, the objective is to get only the transmittance of the samples being analyzed. However, the filter media influences the results obtained for the sample spectrum. In order to eliminate or mitigate the filter

media influence, a background spectrum is taken before the sample transmission. This background is taken using a blank filter that is not exposed to dust. The FTIR instrument is capable of dividing the background blank filter spectrum from the spectrum generated for a filter containing sample. According to (Pampena et al., 2020), the blank filter should be selected from the same batch of filters to be used in the experiments on a specific date. Figure 10 shows the basic steps for acquiring the transmission spectra for a sample. As mentioned, the chamber is purged every time it is opened (shown in the second image), the blank filter background is taken using a blank filter from the same batch of the filters used for sampling, and then the sample spectrum is taken using the loaded filter (shown in the first image).

Figure 10: Transmission spectrum acquiring procedure.

After the background transmission is removed from the actual sample transmission, some filter media interference might still happen. There is a variability on the transmission spectra from filter to filter, even when they are from the same production lot. Therefore,

the transmission from the blank filter used as background may be different from the transmittance of the unexposed filter to be used later for sampling. The difference in transmission for filters from the same lot can be explained due to differences in the filter media itself, differences in the purging time and its effectiveness, contamination of the filter with undesired particles, damages to the filter structure during handling, and the displacement of the filter in the filter holder. Further studies need to be carried out to understand the influence of these aspects on the variability of transmissions for filters from the same batch. This variability can be mitigated or eliminated by applying a normalization process. Figure 11 shows transmission spectra taken for seven blank filters from the same batch. As we can see, the transmission spectra vary considerably for the blank filters from the same batch, reaffirming the need for a normalization procedure.

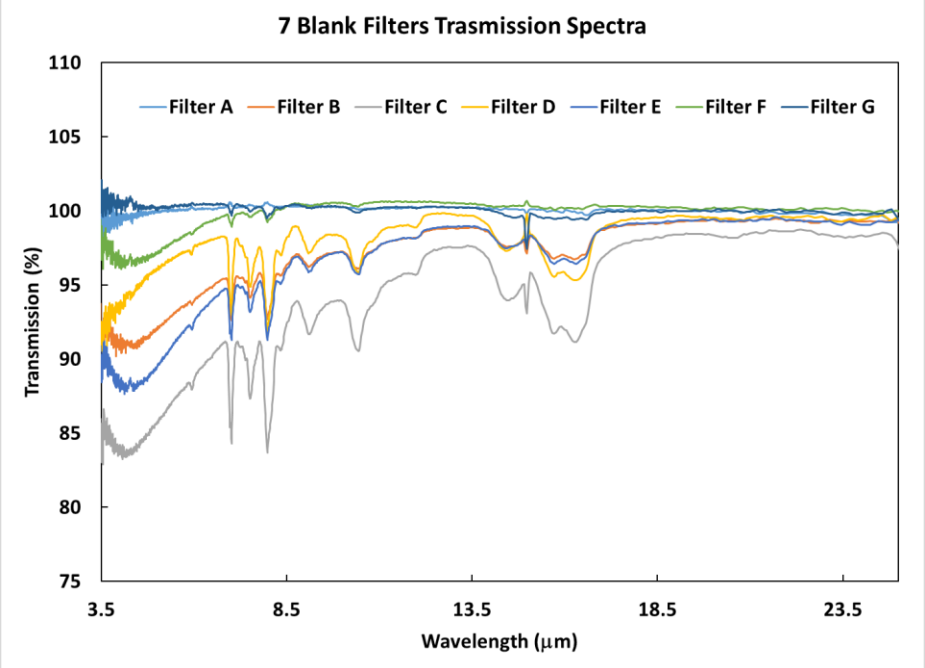

Figure 11: Blank filters transmission spectra for the November, 09th, 2020 batch.

Currently, the transmission spectra have been normalized using two different approaches. The first method is only applied to silica spectra and consists of using linear interpolation for normalizing the transmittance. The second normalization approach consists of using a reference transmission of the filters before they are exposed to dust. These two methods for normalizing the spectra will be discussed in the following sections.

2.4.3.1 Linear Interpolation Normalization Procedure

When quantifying silica mass concentration, the normalization of the transmission spectra can be performed using linear interpolation on the transmission spectrum. This step is performed after the silica transmission spectrum is generated, already having removed the background spectrum from a blank filter. It is important to mention that the interpolation procedure provides a good response for samples that contain only silica.

The linear interpolation normalization is conducted through calculations with Excel using the data generated from the FTIR measurements of the loaded filters. Once the FTIR data is read into Excel, which contains the wavenumber and the transmission columns, the wavenumber is converted into wavelength. A plot is then generated based on the wavelength and the transmission values. The wavelength is then limited to a range of 12 to 13 microns, which is the range that presents the two characteristic area peaks for quartz. The normalization is made based on the linear interpolation of the straight line generated from the transmission values of the wavelength limits applied, respectively 12 and 13 microns. For each point in the spectrum, a value of transmission is calculated by applying linear interpolation using the equation:

$$T_c = T_1 + \frac{(\gamma_c - \gamma_1) * (T_2 - T_1)}{(\gamma_2 - \gamma_1)}, \qquad \textit{Equation 4}$$

where the value of T_c is the calculated transmission for the given $\gamma_c$wavelength. The values of γ_1 and γ_2 are respectively 12 and 13 microns, and the values of T_1 and T_2 are the transmissions measured associated with γ_1 and γ_2 wavelengths. Figure 12 shows the linear interpolation normalization procedure applied for a silica spectrum, having the wavelength limited to a 12 to 13 μm range.

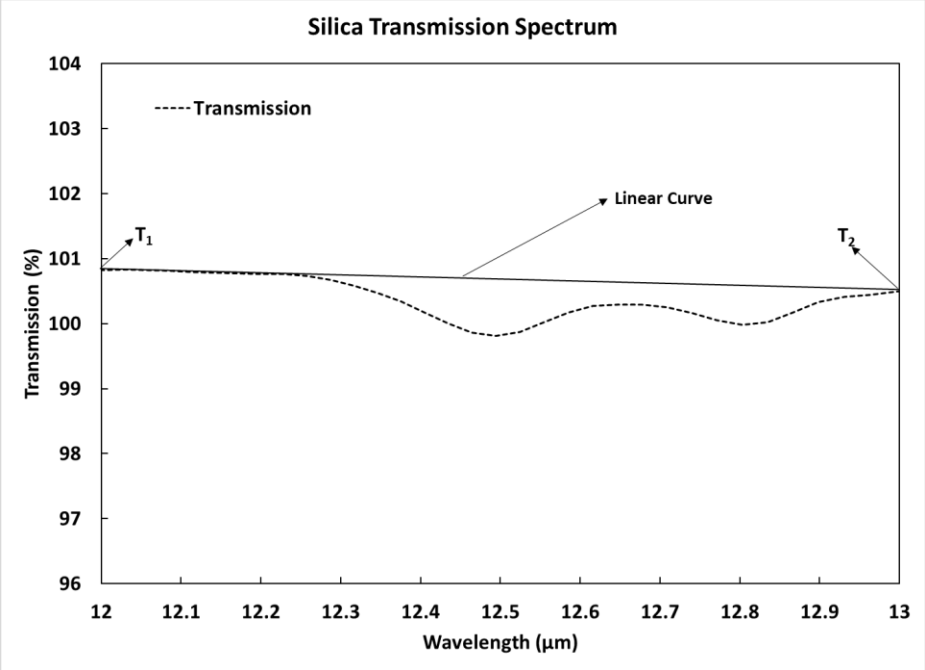

Figure 12: Silica transmission spectrum with linear curve for normalization.

After proceeding with the interpolations, the normalized transmission is obtained by dividing the original transmission measured with the FTIR by the transmission calculated by interpolating each wavelength. According to (Wei et al., 2020), applying a normalization procedure guarantees that the FTIR transmission spectrum reflects only the mineral dust sample transmittance.

2.4.3.2 Reference Spectra Normalization Procedure

The reference spectra normalization procedure is a method applied to normalize the transmission spectra for any dust sample. This procedure for normalization consists of acquiring reference spectra for the filters that will be used to collect sample. Prior to being exposed to the dust plume, the filters are labeled and taken to the FTIR instrument for transmission measurements. The same steps for background removal are taken with the pre-exposed filters. For each blank filter to be loaded with samples, a transmission spectrum is taken and the background transmission is removed using the standard blank filter for that specific batch. The spectra generated are saved for posterior normalization. Once the same filters are exposed to the dust plumes and the samples are collected, they are taken to the FTIR instrument for another round of transmission measurements. This time, the transmission spectra taken will translate the transmittance of the samples. The background transmission of the standard blank filter needs to be removed one more time before taking the transmission spectra of the loaded filters.

The normalized transmission is obtained by dividing the transmission generated post-exposure by the transmission generated pre-exposure, both having the background transmission removed during the measurements in the FTIR.

Although in some cases the step described above will be sufficient to normalize the transmission spectra, it does not happen in most of the cases studied. The variability of the transmission for the reference filters is such that it may change from measurements that are taken even on the same day or taken on different days for the same filter. This variability will result in an inadequate normalized transmission spectrum. To overcome

this shortcoming, the reference transmission can be revised by assigning a correction factor to it. This factor is extremely sensitive and will vary from filter to filter.

The photoacoustic absorption spectrum is used to guide the normalization procedure by identifying a wavelength with zero absorption. The absorbance in the FTIR absorption spectrum also needs to be equal or close to zero at the specific wavelength. It is important to notice that when applying the correction factor, the calculated absorption using the normalized transmission should not be negative.

To justify the use of the correction factor, several spectra for the same filter were taken to demonstrate the variability of the transmission for the reference filter. Figure 13 and Figure 14 show the different spectra taken for the same blank filter that would be later used for dust sampling. As shown, 6 transmission spectra were taken, on each day, for the same reference filter. The spectra vary considerably, and it can be a result of changes on the filter media, difference in the purging, and the filter placement in the filter holder. The correction factor is, therefore, a factor that can account for the variability of the reference filter when normalizing the sample spectrum. If the correction factor is not applied, when needed, the concentration can be overestimated, in most of the cases studied.

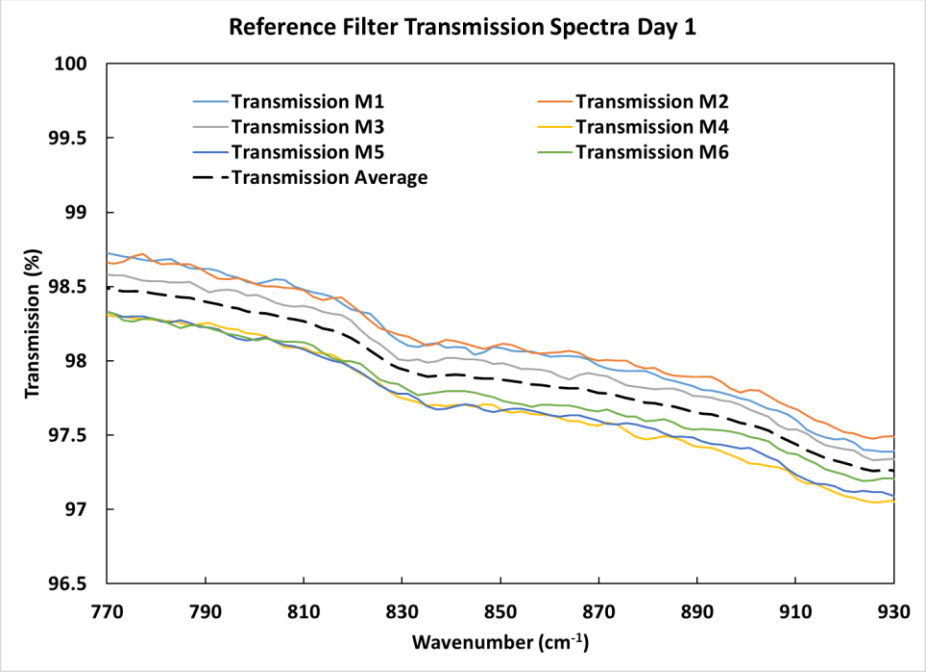

Figure 13: Variability of transmission spectra for reference filter on day 1.

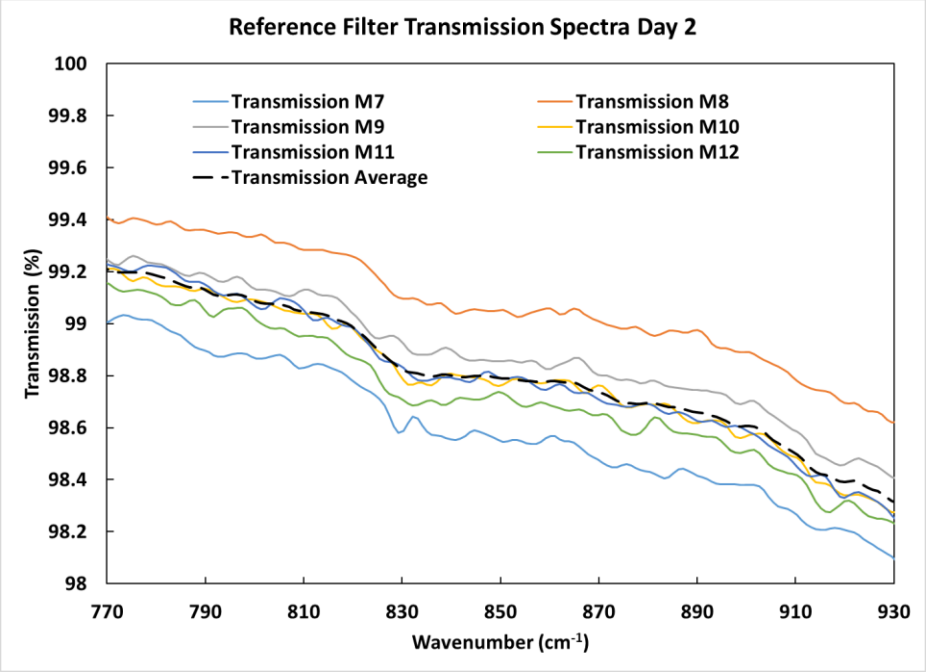

Figure 14: variability of transmission spectra for reference filter on day 2.

Figure 15 presents the reference transmission, the sample transmission, and the revised reference transmission for a mixture of kaolinite and silica. As shown, the revised

reference transmission, after applying a correction factor of 1.008, had the variability of the filter media mostly removed. That can be seen in the range of 12 to 12.5 microns where there is no absorption for the given sample, but only the filter media itself. At this range, the revised reference filter transmission and the sample transmission match.

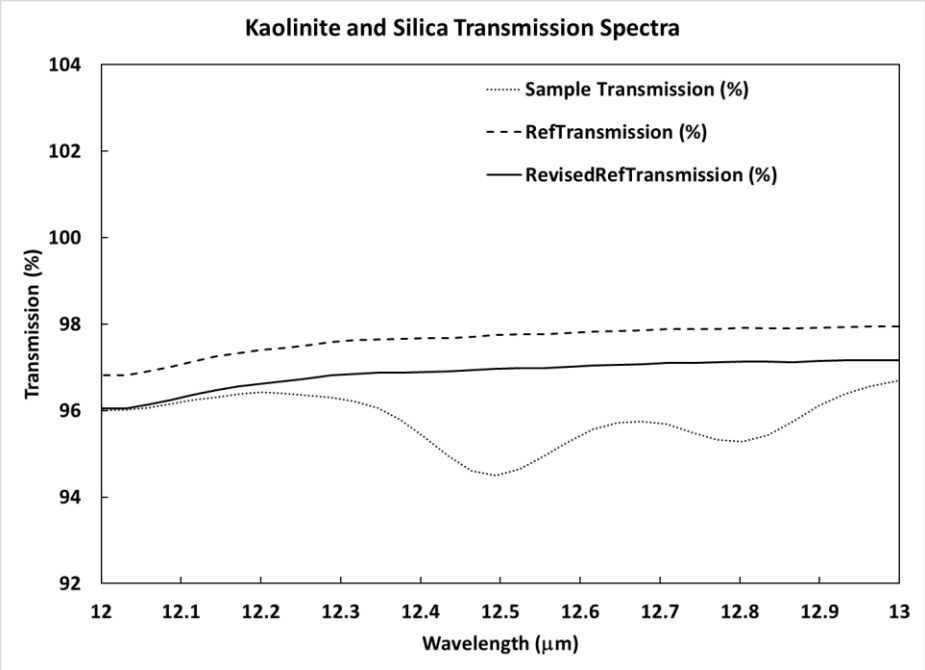

Figure 15: Kaolinite and silica transmission spectra.

2.4.4 Absorption Spectra

After being normalized, the transmission spectra need to be converted into absorption. This step is crucial for calculating the mass concentration of a sampled dust, either using the mass absorption efficiency or the integration of the area under the curve using the NIOSH FAST software, in the case of silica samples. The spectral range will be given in the next section.

The absorption coefficient (Babs) spectra for a mineral dust are obtained by transforming the transmittance into absorbance, and are used to compare FTIR measurements with photoacoustic measurements. The calculations are based on the attenuation (ATN), area of filter exposed to sample deposition (A) in cm^2, sampling flow rate (Q) in LPM, and duration (t) in minutes. The attenuation is calculated as the negative natural logarithm of the normalized transmission. The following equation is used to perform the transformation (Arnott et al., 2005).

$$Babs = \frac{ATN * A * 100000}{Q * t} \qquad \textit{Equation 5}$$

Based on the absorption coefficient and the mass absorption efficiency (MAE), the mass concentration can be calculated. Another way to calculate the mass concentration, when treating a silica sample, is by applying the NIOSH FAST software, which is capable of determining the silica concentration based on the integration area under the absorption curve for the characteristic peak areas. This method for determining silica concentration will be explained in detail in the next subsection.

2.4.5 FAST Software

The determination of RCS concentration during the shift is carried out by using the NIOSH Field Analysis of Silica Tool (FAST), which receives data from a FTIR spectroscopy instrument after the area of interest in the spectra is integrated. The software then translates it into a silica mass and a silica concentration based on the sampling time and pump flow rate for each sample collected (Pampena et al., 2020). The integration of the spectrum areas of interest are usually performed by the FTIR instrument analyst software.

The FAST software also supports importing a generic .CSV or .XLSX file, and it should be used when the integration of the areas for the minerals of interest are not performed using one of the macros mentioned previously. The mandatory fields for the generic excel file are the same: sample name, Q, K, M, D, and C. For this project, the integration area of the quartz signature feature was performed on Excel and the value of Q was input into FAST.

Once the normalization of the transmission spectrum for the loaded filter is performed, the absorbance for each wavenumber is calculated using the following equation.

$$Absorbance = -log10(\frac{Normalized\ Transmission}{100}) \qquad \textit{Equation 6}$$

The most characteristic absorbance peak area for quartz is found in the wavenumber range of 815 cm^{-1} and 770 cm^{-1}, and it is maximum peak is at the wavenumber of 800 cm^{-1} (MSHA P7, 2021). The quartz derivative absorbance (Absorbance dwavenumber) for the wavenumbers in the range 815 cm^{-1} to 770 cm^{-1} is calculated using the following equation.

$$Absorbance\ dwavenumber(i) = Absorbance * \big(wavenumber(i) - wavenumber\ (i-1)\big) \qquad \textit{Equation 7}$$

This equation is used to calculate the differential area under the curve for each pair or wavenumbers in the range of the quartz peak area. The value of Q is obtained by adding all the Absorbance dwavenumber for the range of 815cm^{-1} to 770cm^{-1}. Once Q is calculated, it is manually input into the FAST software. Similarly, the value of K can be determined by adding all the Absorbance dwavenumber for the range of 930 cm^{-1} to 900 cm^{-1}. For samples that contain both silica and kaolinite, the value of K can also be manually

input into the FAST software. The NIOSH FAST will then remove the kaolinite interference on the quartz peak area of 815cm^{-1} to 770cm^{-1}. As shown in Figure 16, the fields for calculating the silica mass and concentration are filled out based on the filter sampling specifications and the quartz absorbance. It is important to mention that in FAST it is only possible to input an integer number for the sampling time/duration.

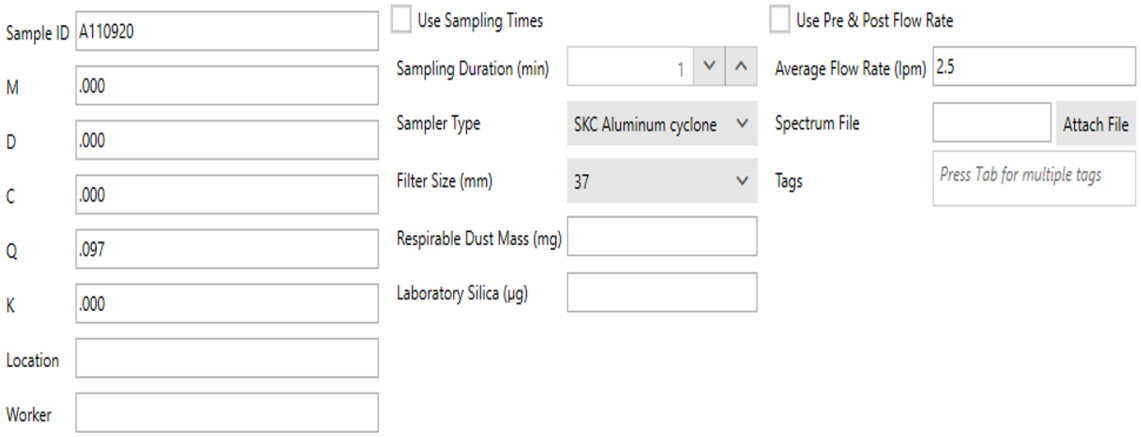

Figure 16: FAST parameters for silica mass concentration calculations.

3 FTIR Spectra

In the UNR aerosol testing chamber, several experiments have been performed for dust monitoring. The filter sampling method applied, coupled with the transmission measurements using the FTIR, allowed the generation of absorption coefficient spectra for different dust materials, which include silica, kaolinite, coal, and a mixture of them. Figure 17 presents a FTIR silica absorption spectrum for a sampled filter that was loaded on November 9th, 2020, with a sampling time of 1.77 minutes and a flow rate of 2.5 liters per minute. The dust dispersal system was loaded with ¼ tsp of silica powder. The

spectrum shows an agreement with the theoretical absorption spectrum for silica, with two characteristic peaks at 12.44 and 12.8 μm.

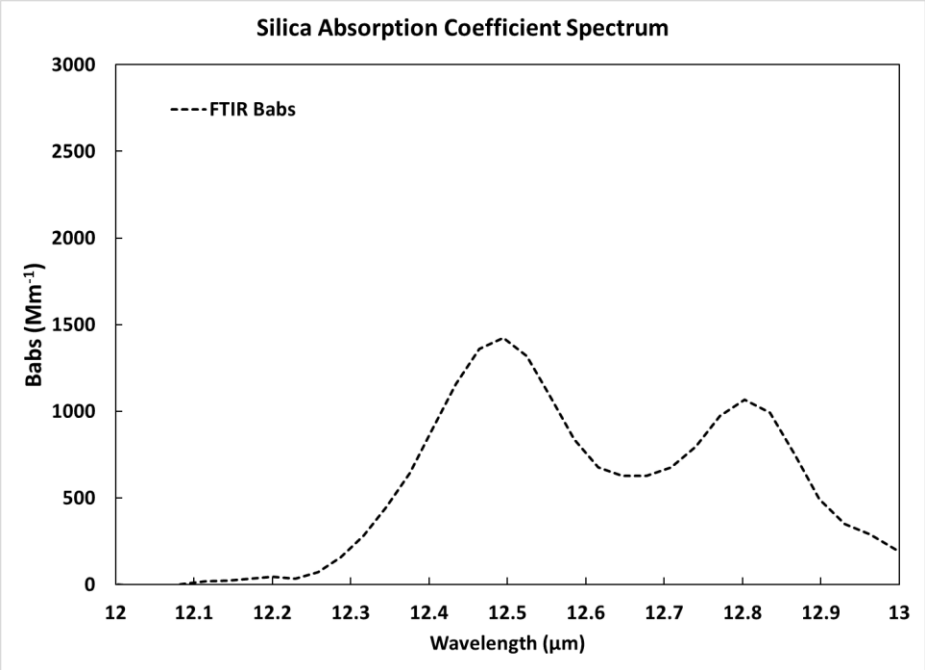

Figure 17: FTIR Absorption coefficient spectrum for silica.

Figure 18 presents a FTIR kaolinite absorption coefficient spectrum for a sampled filter that was loaded on March, 5th, 2021, with a sampling time of 3 minutes and a flow rate of 2.5 liters per minute. The dust dispersal system was loaded with ¼ of tsp of kaolinite powder. Although the FTIR can cover a wider range for the wavelength, the range shown will match the QCL wavelength limits. As shown in the plot, the spectrum matches the theoretical spectrum for kaolinite for the given wavelength range, presenting the increase of absorption at 11 μm and the peak area at the 12.5 μm. The latter is also the most characteristic peak area for quartz and is where kaolinite interfere in the calculation of silica mass concentration.

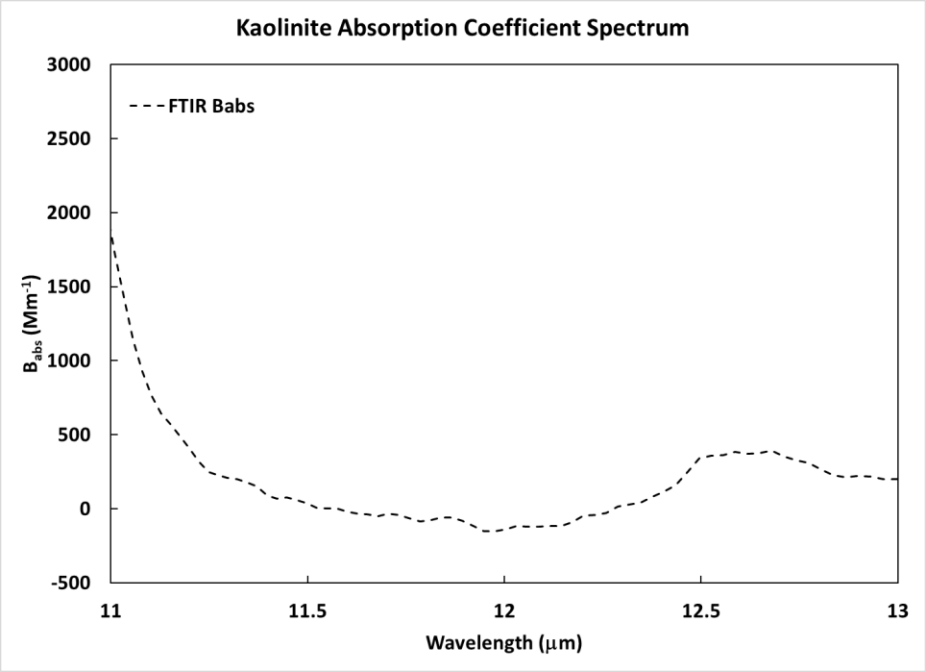

Figure 18: FTIR absorption coefficient spectrum for kaolinite.

Figure 19 presents a FTIR coal absorption coefficient spectrum for a sampled filter that was loaded on March 5th, 2021, with a sampling time of 3 minutes and a flow rate of 2.5 liters per minute. The dust dispersal system was loaded with ¼ of tsp of coal powder. The spectrum shows that coal is absorbed through the entire range of 11 to 13 μm. As shown in the figure, the coal spectrum is relatively featureless and does not present characteristic peaks when compared to the kaolinite and silica spectra. Finally, figures 20 and 21 present the FTIR absorption coefficient spectra for a mixture of silica and kaolinite, and silica and coal. Figure 20 shows the silica and kaolinite spectrum for a sampled filter that was loaded on March 22nd, 2021, with a sampling time of 3 minutes and a flow rate of 2.5 liters per minute. The dust dispersal system was loaded with 1/8 of tsp of kaolinite and 1/8 of tsp of silica powder. It is possible to notice the presence of kaolinite around the 11 and 11.4 μm.

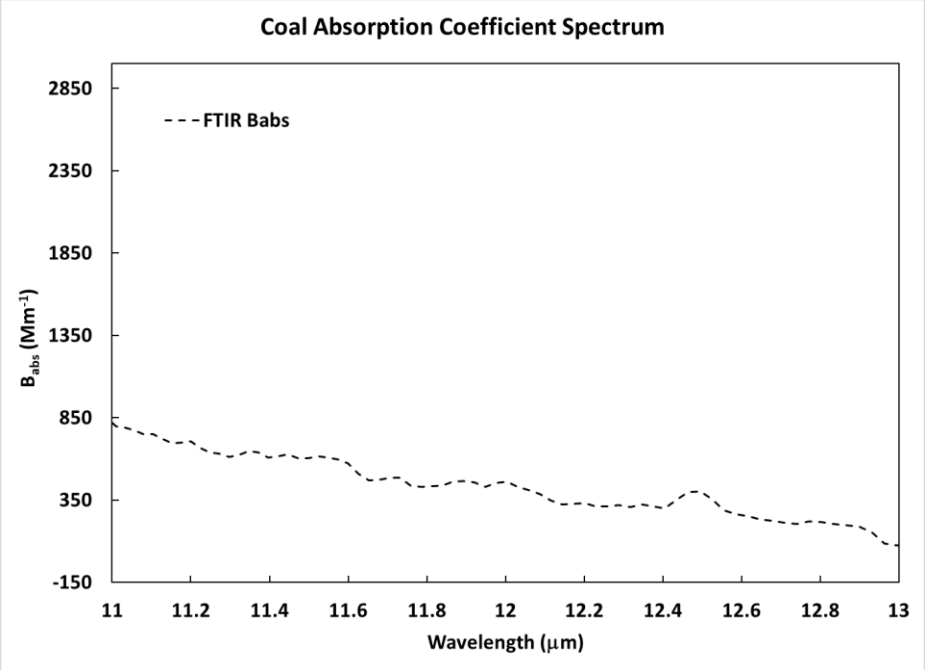

Figure 19: FTIR absorption coefficient spectrum for coal.

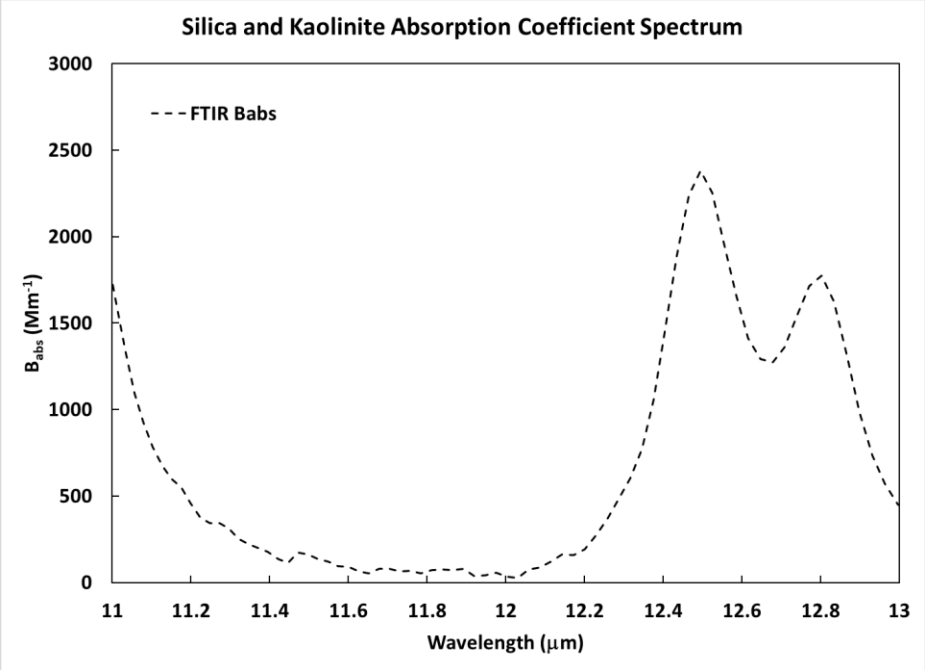

Figure 20: FTIR absorption coefficient spectrum for a mixture of silica and kaolinite.

Figure 21 shows the silica and coal spectrum for a sampled filter that was loaded on November 2nd, 2020, with a sampling time of 2 minutes and a flow rate of 2.5 liters per

minute. The dust dispersal system was loaded with 1/8 of tsp of coal and 1/8 of tsp of silica powder. Since coal is absorbed throughout the range of 12.3 to 13 μm and does not present a characteristic peak, the absorption coefficient spectrum for the mixture of silica and coal looks similar, in shape, to the absorption coefficient spectrum for silica.

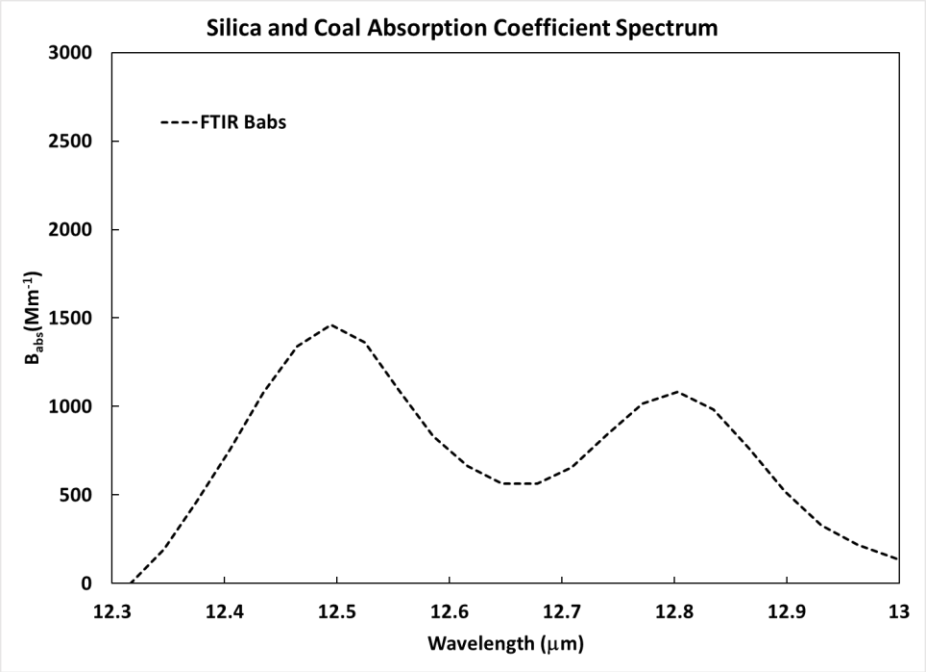

Figure 21: FTIR absorption coefficient spectrum for a mixture of silica and coal.

4 paQCL and FTIR Spectra

During each experiment in the dust testing chamber, the cyclone sampler and the photoacoustic instrument were applied to later compare the results between the two techniques. The following figures display the different spectra generated with the data from the FTIR (curves are named FTIR Babs) and the photoacoustic instrument (curves are named QCL Babs). The spectra generated by the photoacoustic instrument will present water vapor and CO_2 absorption peaks that are not shown in the FTIR spectra. The reason

is the use of a purging system in the FTIR instrument, which allowed for the removal of H_2O and CO_2 interferences, and because the filter concentrates aerosol. Figure 22 shows the silica absorption coefficient spectra for both techniques. The two spectra follow the theoretical spectrum for silica, presenting the two characteristic peaks for the range of 12 to 13 μm.

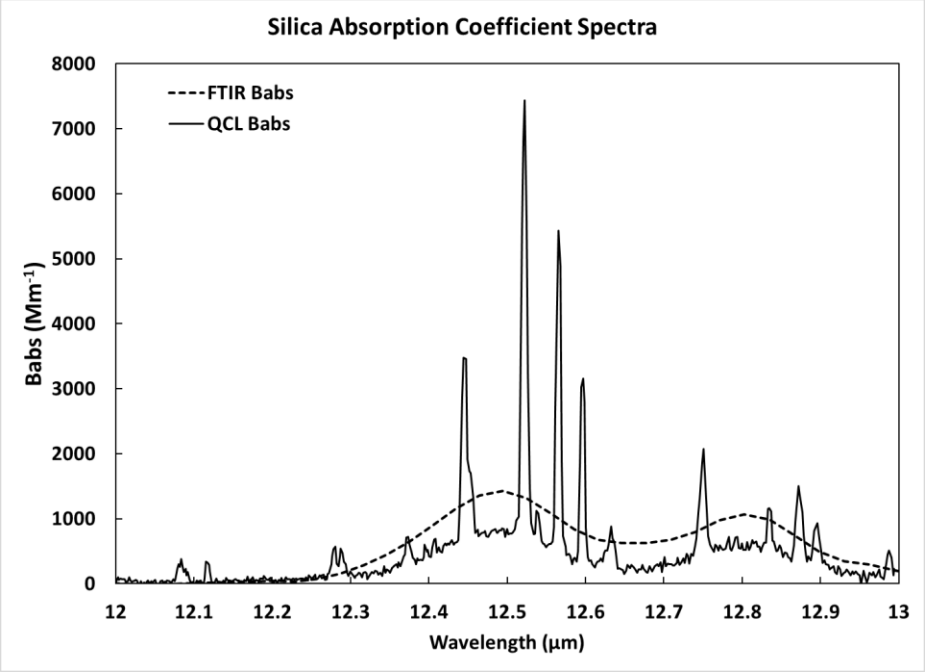

Figure 22: FTIR absorption coefficient spectrum for a mixture of silica and coal.

Although both spectra follow the theoretical absorption coefficient spectrum shape for the studied wavelength range, it is noticeable that the FTIR Babs spectrum presents higher absorption coefficient when compared to the QCL Babs spectrum. The monitoring of dust in suspension is different than the techniques applied with dust collection onto filters. The main difference is faced during the spectrum measurements. A phenomenon described as scattering and absorption enhancement happens when taking transmission

measurements on loaded filters. The light is partially scattered in the filter media structure, which increases its absorption. This phenomenon explains why the FTIR absorption coefficient spectrum is higher than the photoacoustic Babs, which is measured with dust in suspension (Arnott et al., 2005).

Figure 23 presents the absorption coefficient spectra for kaolinite. As shown, the spectra remarkably agree at the range of 11 to 12 μm. However, at the range of 12 to 13 μm, the photoacoustic instrument does not indicate much absorption by kaolinite.

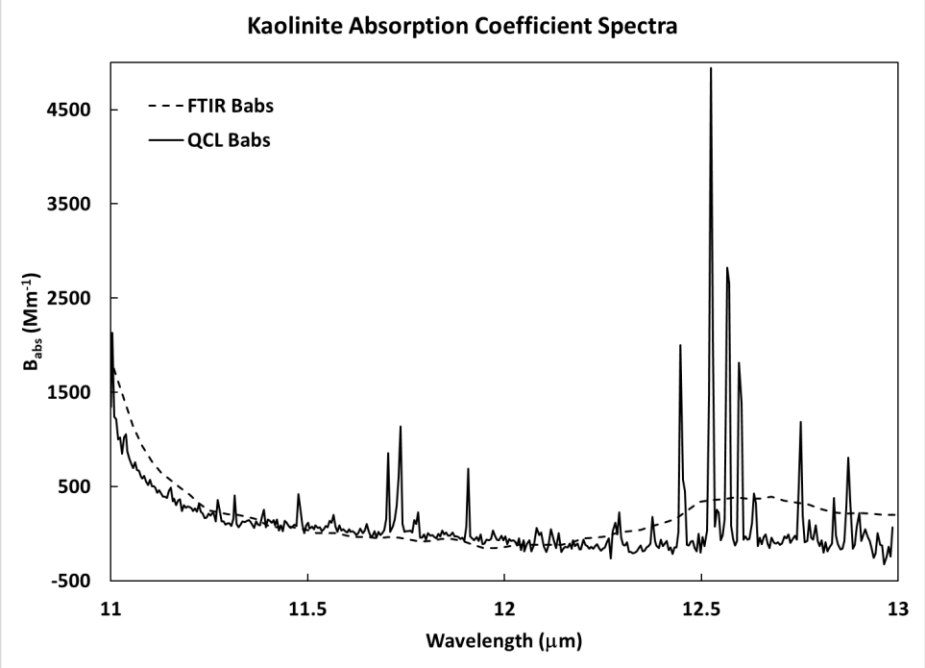

Figure 23: FTIR absorption coefficient spectrum for a mixture of silica and coal.

Figure 24 shows the absorption coefficient spectra for coal. The FTIR and paQCL spectra follow the theoretical absorption spectra for coal, in the range presented in the plot. However, between 12 and 13 μm, the photoacoustic instrument does not present absorption for coal, but only water vapor and CO_2.

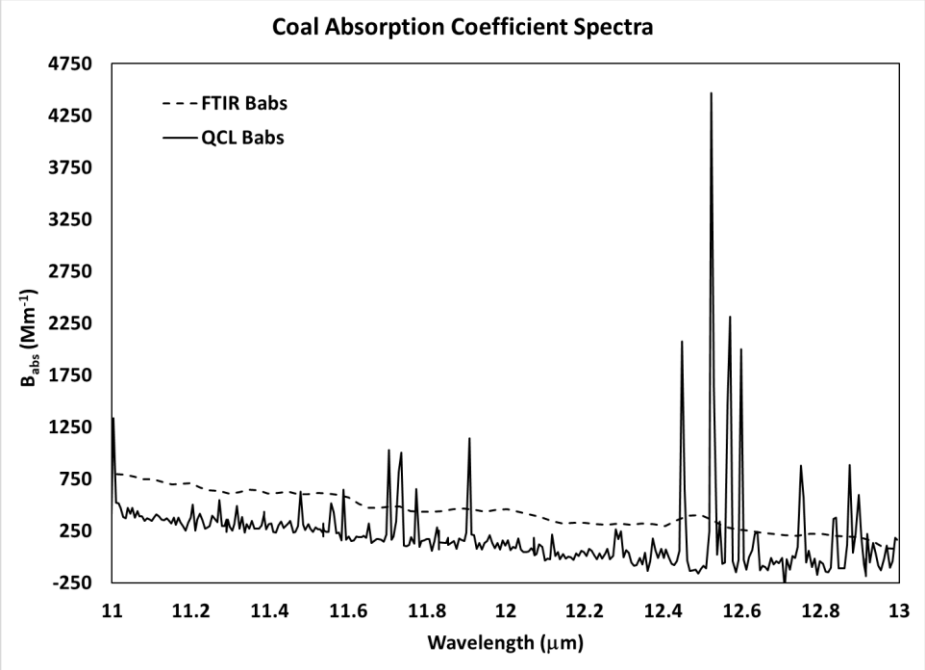

Figure 24: FTIR absorption coefficient spectrum for a mixture of silica and coal.

Figure 25 shows the absorption coefficient spectra for a mixture of silica and kaolinite. The spectra agree remarkably between them and with the theoretical spectra for kaolinite and silica. As shown in the plot, the absorption increases around the 11.2 μm to 11 μm which is characteristic of kaolinite. The silica characteristic peak, containing kaolinite influence, is shown between 12.2 and 13 μm.

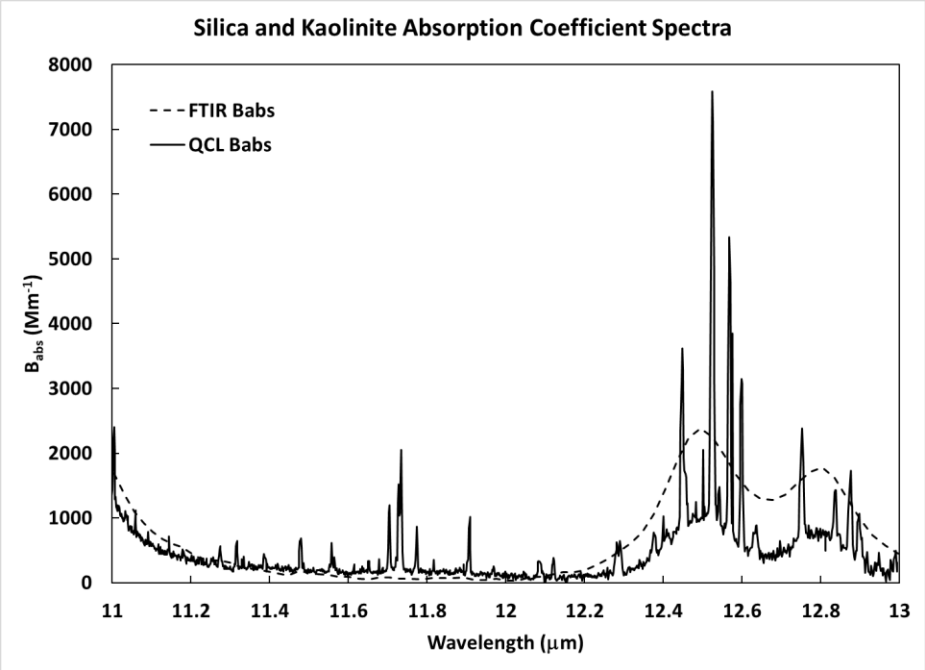

Figure 25: FTIR absorption coefficient spectrum for a mixture of silica and coal.

Figure 26 shows the absorption coefficient spectra for a mixture of coal and silica. The FTIR and QCL Babs curves follow the theoretical spectrum for silica, presenting the two characteristic peaks in the range of 12.3 to 13 μm.

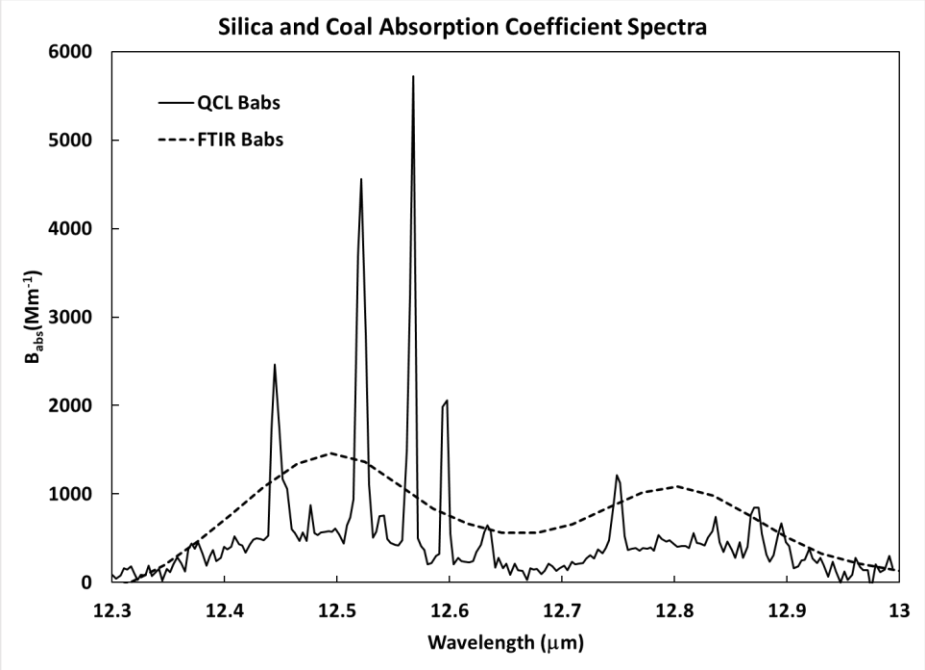

Figure 26: FTIR absorption coefficient spectrum for a mixture of silica and coal.

5 APS and SPS30 Data

Figure 27 shows the APS and SPS30 mass concentration time series for a silica experiment carried out on October 26th, 2020. The aerosol dispersal system was loaded with ¼ tsp of silica powder. As we can see from the plot, the PM4time series measured by the two instruments remarkably agree. The APS is a well-known and used instrument for concentration measurements. However, the SPS30 is a more compact and much less expensive concentration monitoring instrument. The data collected shows that the results obtained using the SPS30 are reliable when compared to a more "standard" monitoring instrument.

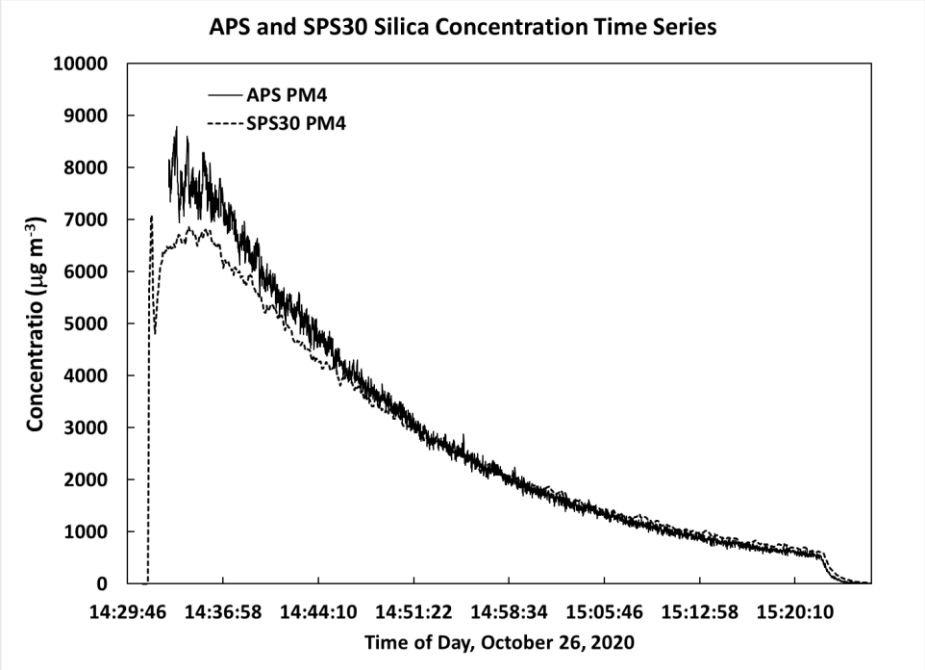

Figure 27: APS and SPS30 data comparison for a silica experiment.

6 FAST Analysis using the NIOSH method

The silica concentration can be calculated using the NIOSH FAST software. The NIOSH FAST can only determine the silica concentration for samples taken in coal mines and can only account for the interference of kaolinite in the silica mass concentration. However, for experiments containing only silica dust, it is possible to acquire the silica mass concentration and compare the results with the mass concentration measured by the SPS30 throughout the experiments. Figure 28 shows the silica concentration time series obtained by the SPS30 instrument for an experiment carried out on November 18th, 2020. For the same experiment, a filter was loaded and taken to the FTIR instrument for transmission measurements. Following the steps described in this manuscript, the silica mass concentration was calculated using the FAST software. As shown in the figure, the

results obtained by the SPS30 considerably match the results obtained by the FAST software.

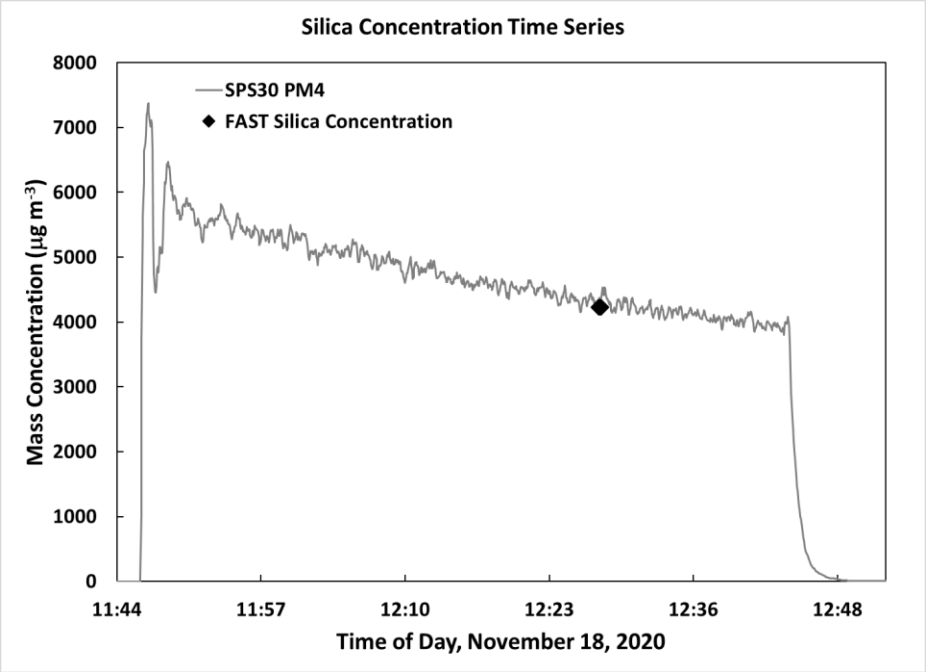

Figure 28: Silica SPS30 PM4 concentration and FAST silica concentration.

Other experiments have been carried out using mixture of silica, kaolinite and coal. Figure 29 shows a silica and coal concentration time series using the SPS30. For this experiment, a mixture of coal and silica was prepared, containing 1/8 tsp of silica and 1/8 tsp of coal powder. Since the FAST software is not capable, at the moment, to calculate the concentration of other minerals, the silica mass concentration for silica was calculated, as an estimation. As shown in the plot, the concentration of silica for a mixture of coal and silica on a filter is lower than the mass concentration measured by the SPS30 for the same time interval. This is an evidence of the presence of coal on the filter, for the SPS30 measures the total concentration of dust in the chamber (silica and coal). The gap between the FAST concentration and the mass concentration measured by the SPS30 can

be considered an estimation of the concentration of coal in suspension in the chamber for the experiment performed.

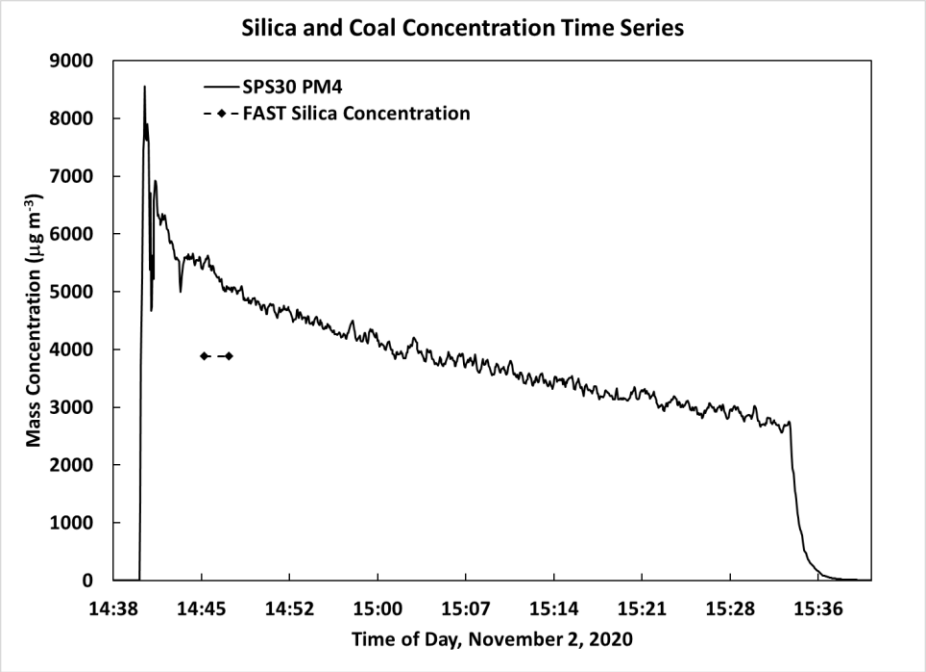

Figure 29: Silica and coal SPS30 PM4 concentration and FAST silica concentration.

Figure 30 shows a time series plot for a silica and kaolinite experiment that was carried out on March 22nd 2021. For this experiment, a mixture of kaolinite and silica was prepared, containing 1/8 tsp of silica and 1/8 tsp of kaolinite powder. The FAST software is capable of accounting for the kaolinite interference in the quartz absorbance peak area. In this case, the Q value (quartz peak area) was calculated for the 815 cm^{-1} to 770 cm^{-1} range and the K value (kaolinite peak area) was calculated for the 930 cm^{-1} to 900 cm^{-1} range. In software, both values were input, and the silica concentration was calculated. As shown in the plot, and similarly to the silica and coal mixture, the silica concentration in FAST is lower than the total dust concentration obtained by the SPS30 for the same

time that the filter was loaded with sample. The kaolinite concentration can be determined as an estimation, using the difference of the concentration measured with the SPS30 and the silica concentration calculated using FAST.

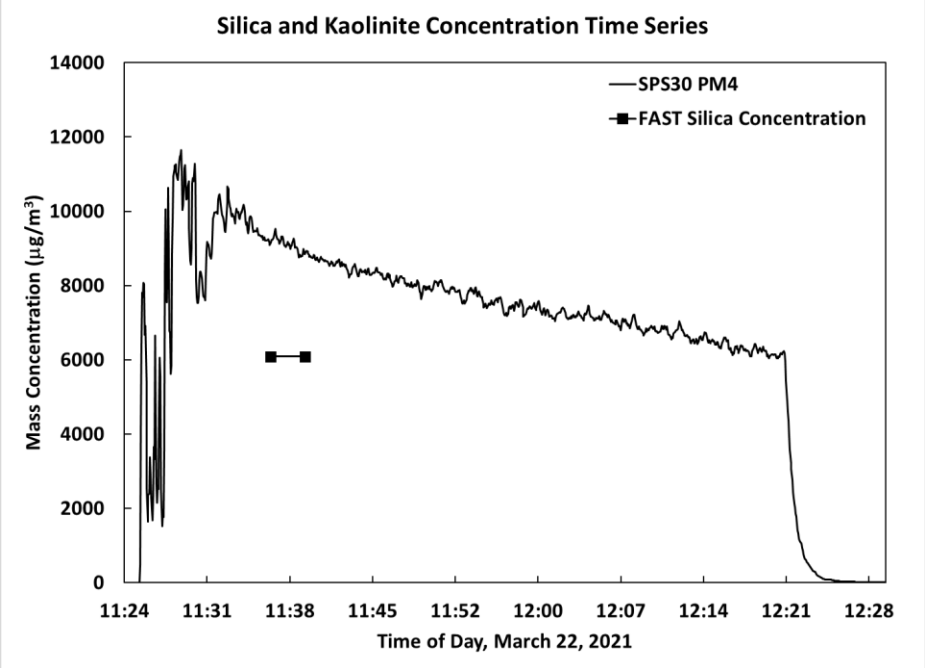

Figure 30: Silica and kaolinite SPS30 PM4 concentration and FAST silica concentration.

7 FTIR FAST Analysis versus PM4 from paQCL Babs

The PM4 calculations from the QCL Babs data requires the use of the Mass Absorption Efficiency (MAE) for the particle. The following equation can be applied to calculate the mass concentration using the absorption coefficient (Babs) and the MAE (Arnott et al., 2005).

$$Mass\ Concentration = \frac{Babs}{MAE}. \qquad \textit{Equation 8}$$

The MAE can be obtained from theoretical curves or empirically. For this manuscript, the empirical MAE is obtained for the mass concentration calculations. The procedure applied

consists of visually matching the PM4 time series curve from the SPS30 data with the absorption coefficient time series curve from the photoacoustic instrument. First, the data from both instruments is plot in the same graph, but on different axes. The inferior limit for the primary and secondary axes is set to zero. The Babs curve is then adjusted visually till it overlaps the SPS30 curve. Once the two curves overlap, the maximum values for the Babs and for the SPS30 are extracted. By dividing the maximum axis scale value for Babs by the maximum axis scale value for the SPS30, the empirical MAE is found.

Figure 31 shows the absorption coefficient spectrum from the photoacoustic and the PM4 SPS30 curve used for calculating the MAE. The Babs time series was obtained parking the QCL laser at the 12.495 μm wavelength.

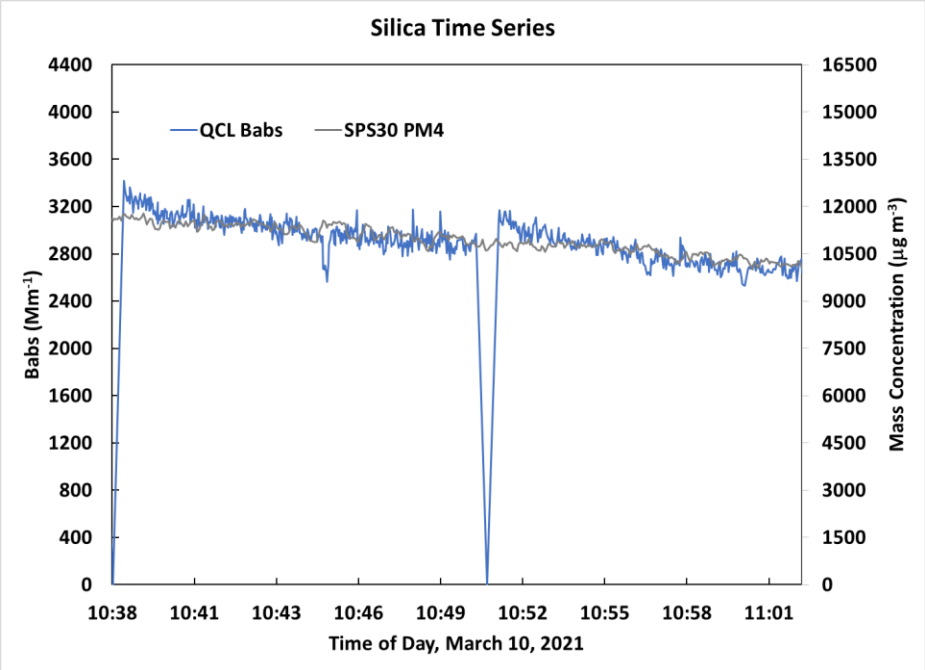

Figure 31: Silica QCL Babs and SPS30 PM4 time series.

It is important to mention that the photoacoustic instrument is zeroing at the beginning time and between 10:49 and 10:52, giving rise to the to the two spikes in this data.

The maximum axis scale Babs value is 4400 Mm^{-1} and maximum axis scale PM4 SPS30 value is 16500 μgm^{-3}. The MAE is then calculated as 0.27 m^2/g. Now, using the MAE empirically calculated, the mass concentration can be determined using Equation 8. The MAE empirically calculated as 0.27 m^2/g is the calibration value that needs to be used in the photoacoustic instrument to obtain silica mass concentration in real time using the absorption coefficient values obtained for the 12.495 μm wavelength. Figure 32 shows the PM4 time series curve determined using the Babs time series and the calculated MAE. The PM4 from the photoacoustic instrument is compared to the SPS30 PM4 and the mass concentration obtained using FAST for two different normalization procedures (linear interpolation and reference transmission). Figure 32 demonstrates the utility of the photoacoustic instrument for measuring silica dust.

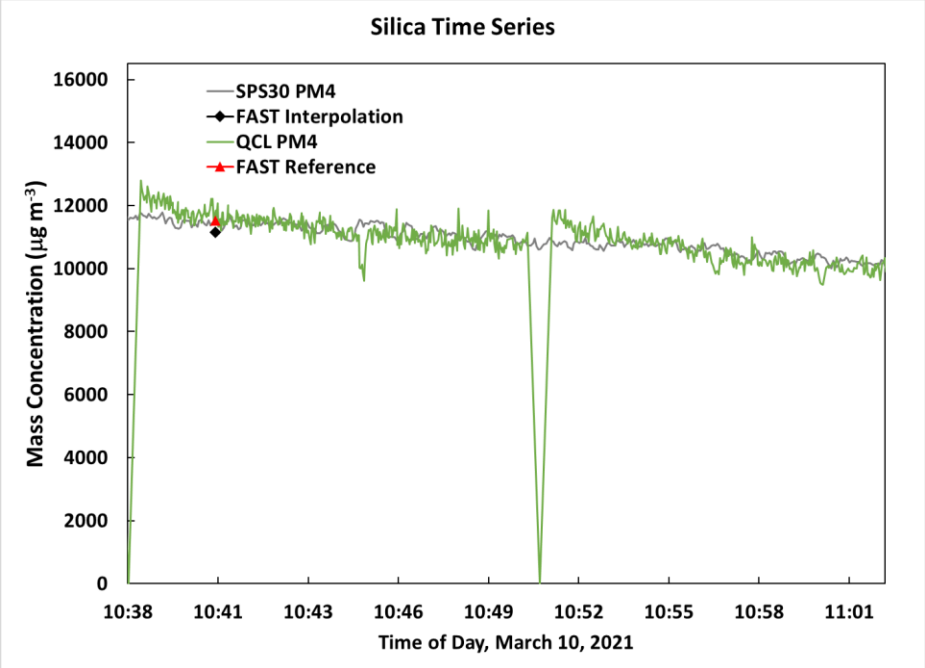

Figure 32: Silica QCL and SPS30 PM4 time series and FAST calculations

8 A Note on Normalization of Transmission Spectra for FAST Analysis

The normalization process is a crucial step for the calculation of dust mass concentration. As mentioned, when a transmission spectrum is not normalized, the calculated absorption can be, in most of the cases, overestimated and the mass concentration of the aerosol sampled will be incorrect. A clear way of showing the effect of the normalization procedure in the mass concentration calculation is achieved when applying the FAST software for silica mass concentration determination.

Figure 33 presents the silica mass concentration calculated in FAST when applying the two normalization procedures on silica samples analysis using the transmission spectrum generated by the FTIR instrument. For the silica experiment carried out with a ¼ tsp of silica, the linear interpolation and the reference transmission normalization procedures were applied. As shown in the plot, the results obtained, for silica experiments, using both normalization procedures are acceptable. The SPS30 mass concentration data was used to validate the results obtained using FAST. The Q value was determined first using the absorbance values calculated using the normalized transmission obtained with the linear interpolation normalization method, and the silica mass concentration calculated in FAST was 11142 $\mu g/m^3$ (shown in the plot with diamond markers). Secondly, the Q value was determined using the absorbance values calculated using the normalized transmission obtained with the reference transmission normalization method, and the silica mass concentration calculated in FAST was 11528$\mu g/m^3$ (shown in the plot with triangle

markers). As shown in the plot, both methods are close to the mass concentration measured with the SPS30. The mass concentration calculated when applying the reference transmission normalization procedure is slightly closer to the SPS30 results.

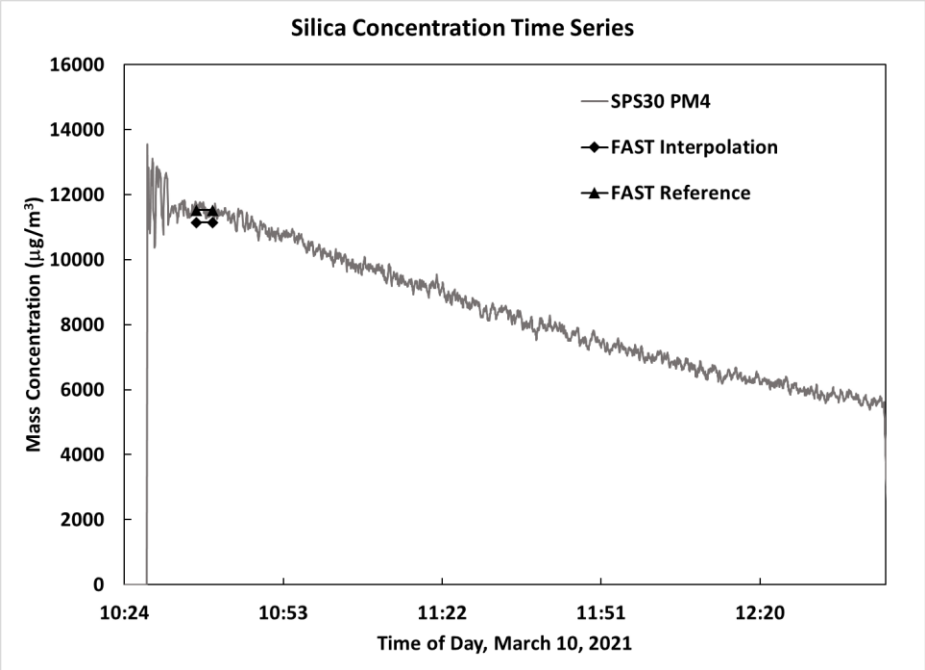

Figure 33: Silica concentration time series for different normalization procedures.

As described in the Methods section, the reference transmission normalization procedure requires, in some cases, the use of a correction factor that is applied to the reference transmission to mitigate or eliminate the variability of the transmissions of a filter. The application of this correction factor is fundamental to obtain reliable results for dust concentration calculations. Figure 34 shows a silica and kaolinite dust concentration time series plot that was generated by the SPS30 for an experiment with a dust mixture containing 1/8 tsp of kaolinite and 1/8 tsp of silica. Based on the transmission spectrum generated in the FTIR instrument and the steps described in the Methods section of this

manuscript, the Q value (integration area for the characteristic quartz peak in the range of 815 to 770 cm^{-1}) and the K value (integration area for the characteristic kaolinite peak in the range of 930 to 900 cm^{-1}) can be determined. For the experiment described, two values of Q and K were calculated. First, they were determined using the non-revised reference transmission spectrum to calculate the normalized transmission – a correction factor was not applied. The Q and K values were respectively 0.468 and 0.349, and the silica mass concentration calculated using FAST was 12000 $\mu g/m^3$ (shown in the plot with the triangle markers). Secondly, a new value of Q and K were calculated using the revised reference transmission after applying a correction factor of 0.8%. The Q and K values were respectively 0.3011 and 0.2424, and the silica mass concentration calculated using FAST was 6086$\mu g/m^3$ (shown in the plot with the square markers).

As shown in the plot, the silica mass concentration for a normalization procedure with a non-revised reference transmission generates an overestimation of the silica mass concentration. That can be proved using the SPS30 data, which provides the total dust concentration in the chamber (silica and kaolinite). The silica mass concentration for the normalization without a correction factor is greater than the total kaolinite and silica mass concentration measured by the SPS30. On the other hand, when the correction factor of 0.8% is applied to revise the reference transmission and account for the variability of transmission of a filter, the silica mass concentration falls under the total concentration measured by the SPS30.

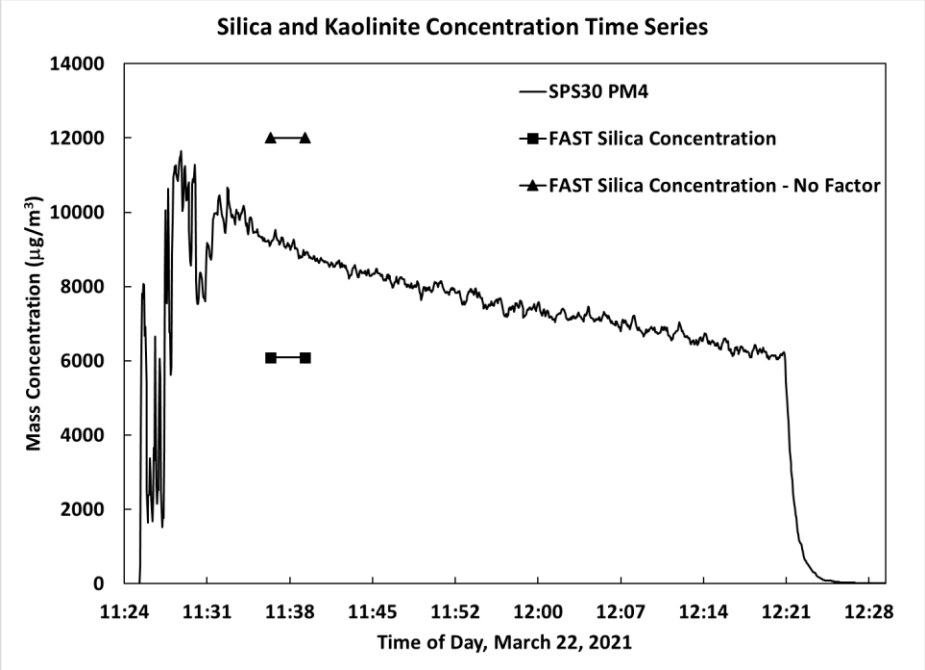

Figure 34: Silica and kaolinite concentration time series for different normalization procedures.

9 Conclusion

9.1 Development of an Aerosol Testing Chamber for Mining Environments Conclusions

The aerosol testing chamber developed at UNR was redesigned for dust monitoring and analysis, which made it capable of emulating underground mine environments, with a dispersal system that allows the generation of different dust plumes, such as silica, coal, kaolinite and mixture of those. The conditions generated in the testing section of the chamber, allows the application of multiple instruments for dust concentration measurements and monitoring and is based on the Marple chamber system installed at NIOSH's Pittsburgh Mining Research Division (PMRD).

9.2 Transmission Spectrum Normalization Conclusions

The normalization of the transmission spectrum has shown to be a crucial step for adequate mass concentration calculations using FAST. As shown in Figures 13 and 14 the variability of the transmission spectra for the same filter is high. The two procedures applied in this manuscript can be used to normalizing the transmission spectrum for silica experiments, as shown in Figure 32. The reference transmission normalization procedure requires the application of a correction factor for revising the reference transmission. This step is crucial because the absorbance of the sample is very sensitive to the transmission value, which can result in an overestimation of a material mass concentration, as shown in Figure 33.

9.3 paQCL and FTIR Spectra Comparison Conclusions

When comparing the paQCL and the FTIR spectra, the immediately noticeable features, as shown in Figures 22 to 26, of the plots are the large spikes created by water vapor and CO_2 in the paQCL absorption spectra. The feature is not present in the FTIR absorption spectra, due to the use of a purging system when acquiring the transmission spectra and because the filter concentrates aerosol. The purging system has shown to be fundamental for the removal of water vapor and CO_2 interference. In Figures 22, 25, and 26, the peaks around 12.4 μm and 12.8 μm are characteristics of silica dust.

Figure 22 shows the silica absorption spectrum as measured by the photoacoustic instrument in-situ. By comparing the paQCL spectrum to the absorption spectrum

obtained by the FTIR, we can conclude that the photoacoustic instrument is capable of quantifying respirable silica in real-time.

The interference of other respirable minerals, such as kaolinite and coal can be present when measurements are taken in the mines. Figures 25 and 26 show the spectra for mixture of theses minerals and, from the theory, it is known that kaolinite and coal can be absorbed at the same wavelength as the characteristic peaks for quartz. However, differently from the FTIR technique, the photoacoustic instrument is capable of measuring the influence of kaolinite and coal.

9.4 SPS30, APS and FAST Software Comparison Conclusions

The mass concentration measurements were carried out using the SPS30 instrument. To validate the data obtained with the SPS30 and justify the use of the instrument, its results were compared to data collected by the APS and also the results from calculations using the NIOSH FAST software. Figure 27 presents the data comparison from the APS and SPS30, and it is noticeable how the two instruments agree. As shown in Figure 28, the results obtained by applying the SPS30 and the NIOSH FAST software methods present a remarkable agreement between them. Additionally, as shown in Figures 28 and 29, for a mixture of silica and kaolinite and silica and coal, the silica mass concentration calculated in FAST is lower than the total mass concentration measured by the SPS30 throughout the experiments. This indicates that the difference between the SPS30 mass concentration and the FAST mass concentration for silica is an estimation of the kaolinite

and coal mass concentrations. Overall, these conclusions suggest that the low-cost air quality sensor SPS30 reliably provides PM4 measurements for RCS experiments.

9.5 FTIR FAST Software Mass Concentration and PM4 from QCL Babs and SPS30 Comparison Conclusions

The agreement between the mass concentration calculated in FAST and the mass concentration obtained with the QCL Babs data, after empirically determining the MAE, is notable. This can be seen in Figure 31. In the same figure, the PM4 for the QCL Babs and the SPS30 is also compared, indicating that the FTIR FAST, PM4 paQCL and PM4 SPS30 mass concentration for silica agree among them. This thesis demonstrates the ability of the new photoacoustic instrument for spectroscopically measuring silica dust concentration in real time, even when other types of dust are present.

10 References

Abu Bakar, N., Cui, H. Z., Abu-Siada, A., Li, S. T., & Ieee. (2016, Sep 25-28). *A Review of Spectroscopy Technology Applications in Transformer Condition Monitoring.* Paper presented at the International Conference on Condition Monitoring and Diagnosis (CMD), Xian Jiaotong Univ, Xian, PEOPLES R CHINA.

Agarwal, Umesh P., & Atalla, Rajai H. (1995). Raman Spectroscopy. In: CRC Press, Inc.

Ampian, S.G., & Virta, R.L. (1992). Crystalline silica overview: Occurrence and analysis. In. Washington, DC: Department of the Interior, Bureau of Mines.

Arnott, W. P., Hamasha, K., Moosmuller, H., Sheridan, P. J., & Ogren, J. A. (2005). Towards aerosol light-absorption measurements with a 7-wavelength Aethalometer: Evaluation with a photoacoustic instrument and 3-wavelength nephelometer. *Aerosol Science and Technology, 39*(1), 17-29. doi:10.1080/027868290901972

Arnott, W. P., Moosmuller, H., Rogers, C. F., Jin, T. F., & Bruch, R. (1999). Photoacoustic spectrometer for measuring light absorption by aerosol: instrument description. *Atmospheric Environment, 33*(17), 2845-2852.

Bajer, Czeslaw I. (2002). Time integration methods - still questions. In (Vol. 1, pp. 45-54). Theoretical Foundations of Civil Engineering.

Berthomieu, Catherine, & Hienerwadel, Rainer. (2009). Fourier transform infrared (FTIR) spectroscopy. In: Springer Science+Business.

Bings, N. H., Bogaerts, A., & Broekaert, J. A. C. (2010). Atomic Spectroscopy: A Review. *Analytical Chemistry, 82*(12), 4653-4681. doi:10.1021/ac1010469

Bunaciu, A. A., Udristioiu, E. G., & Aboul-Enein, H. Y. (2015). X-Ray Diffraction: Instrumentation and Applications. *Critical Reviews in Analytical Chemistry, 45*(4), 289-299. doi:10.1080/10408347.2014.949616

Colinet, J, Listak, J.M., Organiscak, J.A., Rider, J.P., & Wolfe, A.L. (2010). Best practices for dust control in coal mining. In. Information circular (National Institute for Occupational Safety and Health): National Institute for Occupational Safety and

Health, Office of Mine Safety and Health Research.

Cullity, B.D. (1978). *Elements of X-Ray Diffraction* (2nd ed.): Pearson.

Evans, C. L., & Xie, X. S. (2008). Coherent Anti-Stokes Raman Scattering Microscopy: Chemical Imaging for Biology and Medicine. In *Annual Review of Analytical Chemistry* (Vol. 1, pp. 883-909). Palo Alto: Annual Reviews.

Griffith, P.R., & de Haseth, J.A. (1986). Fourier transform infrared spectroscopy. In. Wiley, New York.

Hart, J. F., Autenrieth, D. A., Cauda, E., Chubb, L., Spear, T. M., Wock, S., & Rosenthal, S. (2018). A comparison of respirable crystalline silica concentration measurements using a direct-on-filter Fourier transform infrared (FT-IR) transmission method vs. a traditional laboratory

X-ray diffraction method. *Journal of Occupational and Environmental Hygiene, 15*(10), 743-754. doi:10.1080/15459624.2018.1495334

Johann-Essex, V., Keles, C., Rezaee, M., Scaggs-Witte, M., & Sarver, E. (2017). Respirable coal mine dust characteristics in samples collected in central and northern Appalachia. *International Journal of Coal Geology, 182*, 85-93. doi:10.1016/j.coal.2017.09.010

Jung, J., Yang, J. H., & Yoh, J. J. (2020). An optimal configuration for spark-induced breakdown spectroscopy of bulk minerals aimed at planetary analysis. *Journal of Analytical Atomic Spectrometry, 35*(6), 1103-1114. doi:10.1039/d0ja00057d

Kachuri, L., Villeneuve, P. J., Parent, M. E., Johnson, K. C., Harris, S. A., & Canadian Canc, Registries. (2014). Occupational exposure to crystalline silica and the risk of lung cancer in Canadian men. *International Journal of Cancer, 135*(1), 138-148. doi:10.1002/ijc.28629

Laney, A. S., & Weissman, D. N. (2014). Respiratory Diseases Caused by Coal Mine Dust. *Journal of Occupational and Environmental Medicine, 56*(10), S18-S22. doi:10.1097/jom.0000000000000260

Larkin, Peter J. (2011). *IR and Raman Spectroscopy: Principles and Spectral Interpretation*: Elsevier.

Marple, V. A., & Rubow, K. L. (1983). AN AEROSOL CHAMBER FOR INSTRUMENT EVALUATION AND CALIBRATION. *American Industrial Hygiene Association Journal, 44*(5), 361-367. doi:10.1080/15298668391404978

MSHA. (2013). MSHA P7. In. Pittsburgh, PA: Mine Safety and Health Administration.

MSHA. (2014). *Lowering Miner's Exposure to Respirable Coal Mine Dust, Including Continuous Personal Dust Monitors*. Pittsburgh, PA US: The Mine Safety and Health Administration.

Nascimento, P., Taylor, S.J., Arnott, W.P., Kocsis, K., Wang, X., & Firouzkouhi, H. (2021). *Development of a Real Time Respirable Coal Dust and Silica Dust Monitoring Instrument Based on Photoacoustic Spectroscopy*. Paper presented at the 18th North American Mine Ventilation Symposium, South Dakota School of Mines & Technology.

NIOSH. (1998). *NIOSH 0600 Method*. Cincinnati, OH, USA: The National Institute for Occupational Safety and Health.

NIOSH. (2002). *NIOSH hazard review: health effects of*

occupational exposure to respirable crystalline silica.

NIOSH. (2003a). *NIOSH 7500 Method*. Cincinnati, Ohio: National Institute for Occupational Safety and Health.

NIOSH. (2003b). *NIOSH 7603 Method*. Cincinnati, Ohio: National Institute for Occupational Safety and Health.

NIOSH. (2020). NIOSH Field Analysis of Silica Tool Manual. In: NIOSH.

OSHA. (2013). OSHA's Proposed Crystalline Silica Rule: Overview. In. U.S. Department of Labor: Occupational Safety and Health Administration.

Pampena, J. D., Cauda, E. G., Chubb, L. G., & Meadows, J. J. (2020). Use of the Field-Based Silica Monitoring Technique in a Coal Mine: A Case Study. *Mining Metallurgy & Exploration, 37*(2), 717-726. doi:10.1007/s42461-019-00161-0

Rajavel, S., Raghav, P., Gupta, M. K., & Muralidhar, V. (2020). Silico-tuberculosis, silicosis and other respiratory morbidities among sandstone mine workers in Rajasthan- a cross-sectional study. *Plos One, 15*(4), 15. doi:10.1371/journal.pone.0230574

Schatzel, S. J. (2009). Identifying sources of respirable quartz and silica dust in underground coal mines in southern West Virginia, western Virginia, and eastern Kentucky. *International Journal of Coal Geology, 78*(2), 110-118. doi:10.1016/j.coal.2009.01.003

Shipp, D. W., Sinjab, F., & Notingher, I. (2017). Raman spectroscopy: techniques and applications in the life sciences. *Advances in Optics and Photonics, 9*(2), 315-428. doi:10.1364/aop.9.000315

SKC. (2021). Aluminum Respirable Dust Cyclone. In.

Srungaram, P. K., Ayyalasomayajula, K. K., Yu-Yueh, F., & Singh, J. P. (2013). Comparison of laser induced breakdown spectroscopy and spark induced breakdown spectroscopy for determination of mercury in soils. *Spectrochimica Acta Part B-Atomic Spectroscopy, 87*, 108-113. doi:10.1016/j.sab.2013.05.009

Taylor, S. J., Nascimento, P., Arnott, W.P., & Kocsis, K. (To Be Published). Real-time Photoacoustic Instrument for Mass Concentration Measurements of Respirable Crystal Silica Dust: Theory. In.

Taylor, S.J. (To Be Published). *Development and Testing of a New Airborne Silica Monitoring Technique Based om Photoacoustic Spectroscopy, and Comparison to Current Techniques.* (Master's), University of Nevada, Reno, Reno, Nevada.

Wei, S. J., Kulkarni, P., Zheng, L. N., & Ashley, K. (2020). Aerosol analysis using quantum cascade laser infrared spectroscopy: Application to crystalline silica measurement. *Journal of Aerosol Science, 150*, 13. doi:10.1016/j.jaerosci.2020.105643